Thesis (Summer 2016)

Report on

TIME-INDEPENDENT SCHRODINGER-POISSON COUPLED SIMULATION BASED STUDY OF InP AND InAlAs QUANTUM WELL FIELD-EFFECT TRANSISTORS

Inspiring Excellence

Thesis Group Members:

Mehdi Ahsan ID: 13121029

Abrar Hayat ID: 13121039

Apurba Nath ID: 13121110

Thesis Supervisor: Dr. Mohammed Belal Hossain Bhuian

Thesis Co-Supervisor: Atanu Kumar Saha

DECLARATION

We hereby declare that the thesis titled "TIME-INDEPENDENT SCHRODINGER-POISSON COUPLED SIMULATION BASED STUDY OF InP AND InAlAs QUANTUM WELL FIELD-EFFECT TRANSISTORS" is submitted to the Department of Electrical and Electronic Engineering of BRAC University in partial fulfilment of the Bachelor of Science in Electrical and Electronic Engineering. This is our original work and was not submitted elsewhere for the award of any other degree or any other publication.

Date:

Dr. Mohammed Belal Hossain Bhuian

Thesis Supervisor

_ _

Atanu Kumar Saha

Thesis Co-Supervisor

_ _

_ _

Mehdi Ahsan

ID: 13121029

_ _

Abrar Hayat

ID: 13121039

_ _

Apurba Nath

ID: 13121110

ACKNOWLEDGEMENTS

We would like to thank our supervisor Dr. Mohammed Belal Hossain Bhuian and co-supervisor Atanu Kumar Saha for giving us the opportunity to work on this field. The completion of our thesis would not be possible without their constant support, encouragement and expert advice throughout the thesis process.

We would like to mention a few books which were critical for the knowledge on basic semiconductor devices required for our thesis. Firstly, Quantum Transport (Atom to Transistor) and Lessons from Nanoscience (A Lecture Note Series) by Supriyo Datta. These were very helpful to carry out the simulations. And lastly, Advanced Semiconductor Fundamentals (Second Ed.) by Robert F. Pierret.

We would also like to mention COMSOL® Multiphysics®; a solver and simulation based solver. This software gave us access to many parameters and enabled us make our simulations precise.

TABLE OF CONTENTS

LIST OF FIGURES

LIST OF TABLES

ABBREVIATIONS

FEM	Finite Element Method
C-V	Capacitance-Voltage
FET	Field-Effect Transistor
JFET	Junction Field-Effect Transistor
MESFET	Metal-Semiconductor Field-Effect Transistor
MOSFET	Metal-Oxide Semiconductor Field-Effect Transistor
HEMT	High Electron Mobility Transistor
QWFET	Quantum Well Field-Effect Transistor

NOMENCLATURE

HfO_2	Hafnium(IV) Oxide
$In_xAl_{1-x}As$	Indium Aluminum Arsenide (similar lattice constant as InGaAs but greater bandgap)
InP	Indium Phosphide (Identical to GaAs and most of III-V semiconductors)
$In_{1-x}Ga_xAs$	Indium Gallium Arsenide
GaAs	Gallium Arsenide

ABSTRACT

The electronics industry first started appreciating QWFETs over MOSFETs back in late 2011 due the QWFET's unique wrapped gate around channel structure, which provided better control over threshold voltage and reduced operating voltage.

Our main purpose was to observe the changes in the gate capacitance of QWFETS with InP as the upper barrier compared to InAlAs as the upper barrier. So we devised a Schrodinger-Poisson coupled simulation in COMSOL® Multiphysics®. The Poisson Equation in our simulation was used to determine the conduction band profiles across the geometry and the Schrodinger Equation was used to find the corresponding probability densities of electrons. We performed the above experiments in both doped and undoped conditions with both InP and InAlAs as upper barriers with increasing gate voltages to see the changes. At the end, we could infer that devices with doped variants of both InP and InAlAs as the upper barrier had better yields of gate capacitance than the undoped materials themselves and more importantly doped InAlAs as the upper barrier had much better yields of capacitance than doped InP as the upper barrier.

1. INTRODUCTION

1.1 The development of FET

The field-effect transistor (FET) is a semiconductor device which controls the conductivity of a channel by the electric field applied. These are unipolar, which means they use single-carrier-type operation. The idea of field-effect transistor was first invented in 1926 by Julius Edgar Lilienfield. But the more advanced forms of the FET were not developed until the 1940's. The different forms of FETs, all have a high input impedance. The basic form of a FET consists of three terminals; source, drain and gate. The voltage applied at the gate is responsible for the channel that is created between the source and drain. Higher the gate voltage (V_g), higher the accumulation of charge carriers, more conductive is the channel and hence better conductivity between the source-and-drain for charge flow. Most FETs are made with silicon by using the conventional bulk semiconductor processing techniques and using a single crystal semiconductor wafer as the active region. FETs have played a major role in development in the electronics world. The first improvement was the JFET and subsequently the MESFET, MOSFET, HEMT, QWFET and many more. The JFET (junction field-effect transistor), developed in 1950's, is the simplest FET ever produced. It can basically be used as a switch or an amplifier which uses a reverse biased p–n junction to separate the gate from the body. The MESFET (metal–semiconductor field-effect transistor), developed in 1966, is similar to the JFET; but only a Schottky junction is used instead of a p-n junction. Then came the MOSFET (metal–oxide–semiconductor field-effect transistor). This is a modified version of the MESFET. In this device there are four terminals. There is a body terminal in addition to the source, drain and gate terminals; the main transition being the addition of an oxide layer in the gate terminal. MOSFET is the most common type of FET [1] used in the modern world among the developed FETs. This is due to the minimum current requirement to be turned on whilst delivering a very current to load. This led to inventions of CMOS technology which uses NMOS and PMOS technologies. Many integrated circuits used are made using these. Then in 1979 came the HEMT (high-electron-mobility transistor). This was developed to mainly avoid the heavy doping required in the channel of MOSFETs. Here the junction between materials of different bandgaps is used as a channel, where a quantum well is created and charge

accumulates. The material combination is usually GaAs and InGaAs. Then came the QWFET (quantum well field-effect transistor). QWFETs use quantum tunneling to increase the speed of a transistors and require very low power compared to MOSFETs and HEMTs.

1.2 Junction Field-Effect Transistor

The junction gate field-effect transistor is the simplest form of a FET[19]. It has three terminals: source, drain and a gate and does not require any biasing voltage. The JFET consists of a channel of semiconductor which has a high concentration of electrons and holes. A pn-junction forms on both sides of the channel using a region with doping. The channels can be either n-type or p-type. JFETs have a large input impedance.

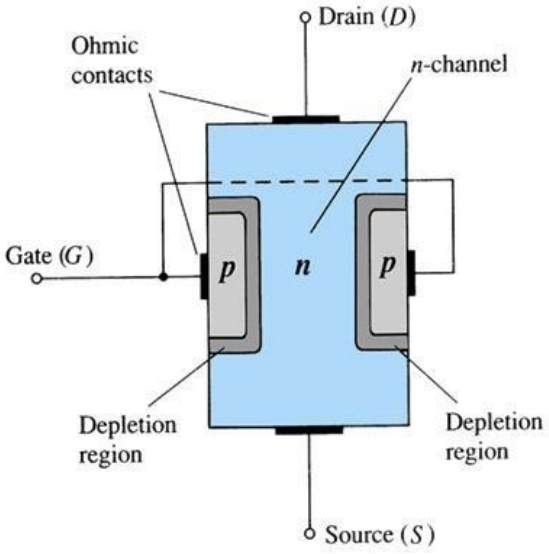

Fig 1.1: A p-doped JFET

In the above figure, we can see a p-doped n-channel JFET. Here, if a negative voltage is applied in the gate terminal, then the depletion region will widen. Hence, the electron flow from drain to source through the n-channel will decrease which means conductivity decreases.

1.3 Metal-Semiconductor Field-Effect Transistor

MESFETs are similar to JFETs; but only a Schottky barrier is instead of a pn-junction. These are faster than JFETs and MOSFETs and hence is more expensive than the other two. In a MESFET if reverse bias is applied in gate-to-source, then a depletion region is created under the gate. Higher the gate-to-source voltage (V_{GS}), lower the current flow.

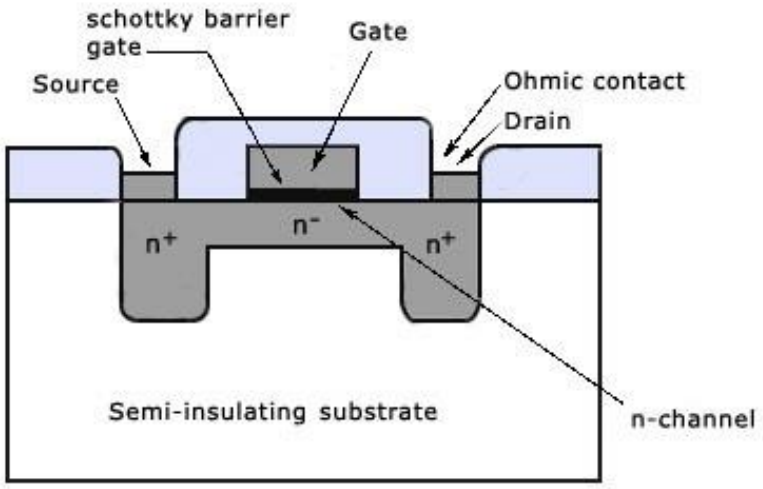

Fig 1.2: An n-channel MESFET

1.4 Metal Oxide Semiconductor Field-Effect Transistor

Metal-oxide-semiconductors field-effect transistors are the most common type of FETs used in the electronic industry. It took over BJTs which were much more common at that time. The construction of a MOSFET is similar to that of a MESFET with an oxide layer on the gate and substrate can be either p-type or n-type. MOSFET is more in use because of the little current required to turn on a transistor whilst providing a higher current to the load. MOSFETS are usually made using silicon but the use of GaAs (gallium arsenide) has increased in the recent years. There are two types of MOSFETS: NMOS and PMOS. NMOS are MOSFETs using an n-channel whereas PMOS are MOSFETs using a p-channel. Electronic circuits are made using a combination of the NMOS technology and the PMOS technology called the CMOS technology. CMOS (complementary metal-oxide semiconductor) has a low power consumption and is relatively cheaper due to the lower number of transistors required. However, one of the disadvantages of MOSFET is that a heavily doped channel leads to reduced carrier mobility. [6]

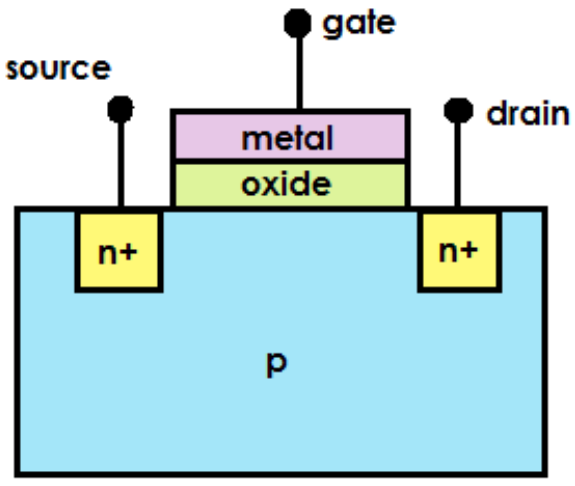

Fig: 1.3: A p-type MOSFET

1.5 High Electron Mobility Transistor

The idea of high-electron-mobility transistor (HEMT) is to create a junction (i.e. heterojunction) between two semiconductor materials with different band gaps to form a quantum well. This quantum well will be used for charge accumulation. The main purpose of a HEMT is to avoid the high amount of doping in the channel that was required in the other FETs. [2] Usually the materials used for the junctions are GaAs and AlGaAs. InGaAs also gives good results. Electrons from the highly doped AlGaAs layer cross the junction and accumulate in a well formed in the GaAs channel. The gate-voltage (V_g) controls the electron concentration inside the well. Higher the gate-voltage, higher will be the electron concentration. This enables electrons to travel from the source to the drain by the channel as scattering is reduced.

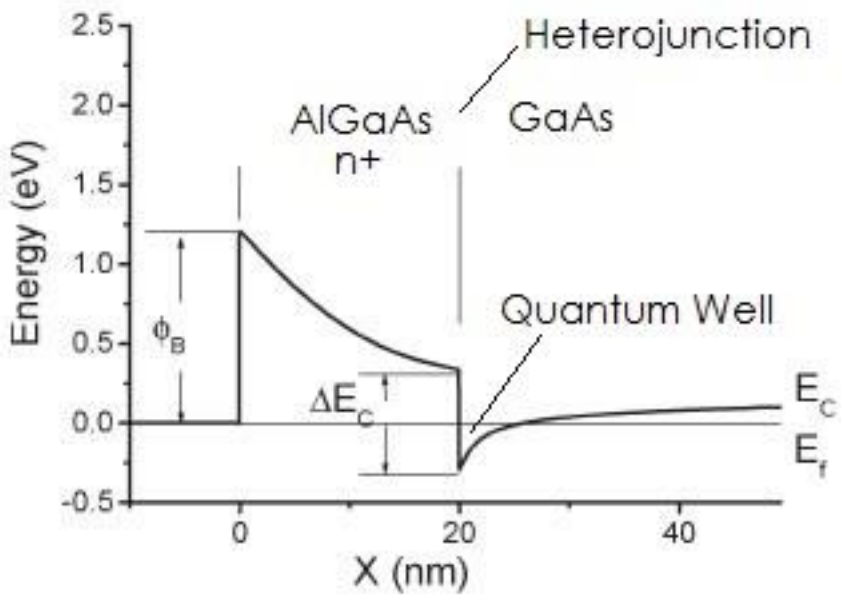

Fig 1.4: A quantum well formed in a heterojunction between AlGaAs and GaAs [5]

1.6 Quantum Well Field-Effect Transistor

These are transistors which use quantum tunneling to increase the speed of the transistors while reducing power consumption. [3] Quantum tunneling is the process were a particle passes through a barrier which is impossible in terms of classical physics. The manufacturing of QWFETs are done by RTP (rapid thermal processing). In this process silicon wafers are heated up to 1000 ^{o}C in matter of seconds and cooled done very slowly to avoid breakage from thermal shock.

QWFETs are similar to HEMTs. QWFETs have two quantum wells compared to HEMTS. The undoped channel is positioned in between two different band gap materials to form two heterojunctions; double heterostructure; which creates two quantum wells. Higher band gaps create higher charge concentration due to high band gaps. Thus making the channel have higher charge accumulation. The electrons are generally trapped in the channels. In a QWFET, as the gate is placed around the channel in more than one side, it is called a multi-gate. [7]

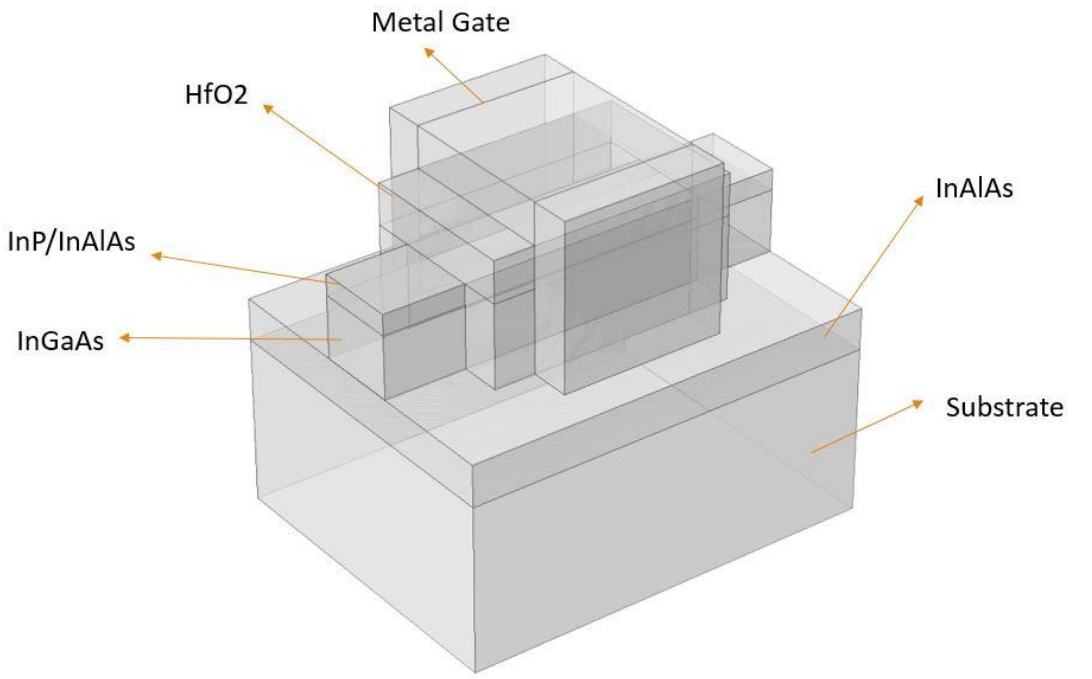

Fig 1.5: A 3D model of a QWFET with a FIN structure

2. SCHRÖDINGER EQUATION

2.1 The importance of using Schrödinger equation

It is easily possible to predict the behavior of a matter by the laws of classical physics. However, in nanoscale, particles start to show wave like properties. Hence the wave-particle duality. In nanoscale, results are obtained such that they cannot be defined by the laws of classical physics. The results obtained, in a larger scale would be similar to that of a tennis-ball passing through a concrete brick wall or a tennis-ball bouncing back from a thin piece of paper. Results also show that an electron may exist in many different positions if a particular experiment is repeated many times; and there is a certain probability for all of these positions. So, Schrödinger equation and Poisson equation combined helps us to determine the probability of the existence in certain states at certain potential barriers.

Schrödinger equation is also an eigen value equation which means it used to calculate the probability of an electron existing in a particular discrete level in a quantum well.

2.2 Schrödinger equation

Schrödinger equation was developed by physicist Erwin Schrödinger in 1925. It is a partial differential equation which has two forms: a) time-dependent and b) time-independent. WE used the time-independent form as our simulations were done in an equilibrium system. This equation is used to find the wave function of a material. The finite element method (FEM) has been used for the calculations. [4][20]

2.3 General Form of a Schrödinger equation

$$E\Psi = \hat{H}\Psi$$

Where, E is the total energy of a system

Ψ is the electron wave function

Ĥ is the Hamiltonian operator

2.4 Time-independent Schrödinger equation

Schrödinger equation for a single non-relativistic particle:

$$E\Psi(r) = [\frac{-\hbar^2}{2\mu}\nabla^2 + V(r)]\Psi(r)$$

Where, E is the total energy of a system

Ψ is the electron wave function

$\hbar$ is the Plank's constant

μ is the effective mass of an electron

∇ is the Laplacian operator

V is the potential profile

3. POISSON'S EQUATION

Poisson's equation was developed by physicist Siméon Denis Poisson[18]. Like Schrödinger equation, it is also a partial differential equation and requires finite element method (FEM) for calculations. Poisson's equation is used to calculate the potential energy field caused by a particular charge or mass density distribution.

General form:

$$\nabla^2 \varphi = -\frac{\rho}{\varepsilon}$$

Where, ∇ is the Laplacian operator

φ is the electric potential energy

ρ is the charge density

ε is the permittivity of the material

4. THE SIMULATION ENVIRONMENT: COMSOL MULTIPHYSICS

4.1 Experience with different simulation environments

As the title of this paper suggests, we aimed to employ a simulation based analysis of the QWFET, and then draw our best possible inferences based on the output of the analysis. Hence, the simulation environment being used is undoubtedly of utter importance, since the reliability and accuracy of the outcomes directly depend on it.

Initially, we had been thinking about the possibilities of using MATLAB to run our simulations. There were several reasons for this consideration. First of all, MATLAB is a distinctively well-known programming language, and is one which is highly acclaimed in the scientific, engineering and the academic community as a whole. Most of the research work we had studied for the purpose of this paper was employed in MATLAB in one way or the other. Due to its massive popularity, code examples and tutorials were readily available online. The MATLAB environment can seamlessly manipulate matrices and also came in with a command-line interface, thus making it a suitable tool for implementing numerical techniques, such as the Finite Difference Method. However, simulating in MATLAB meant designing and coding every aspect of the system from scratch, and we felt that this was somewhat of a repetitive process. We were looking for a simulation environment that would allow us to get started right away, and with minimal effort. Although we were looking for simplicity and ease of use, we were, in no way, ready to compromise performance and accurate approximations to simulated results.

Taking the above factors into consideration, the second simulation environment we planned to resort to was SILVACO®. At the first glance, SILVACO seemed to overcome the limitations MATLAB exhibited. We had also dug up many research papers where SILVACO was employed to simulate semi-classical electrostatics simulations. However, we found the environment to be rather cumbersome and not user-friendly at all. On top of that, tutorials, documentations or any other resources on SILVACO were rarely found.

The third simulation environment we experimented with was COMSOL® Multiphysics®.

COMSOL® Multiphysics® is a solution engine which solves partial differential equations via the finite element method (FEM) for a particular simulation [8]. This is the environment we finally settled for, and the reasons are many-fold. Firstly, as the name "Multiphysics" suggests, COMSOL has the capability to run multiple physics modules for a single simulation, and also allows "coupling" between compatible physics interfaces. This was suitable, since our underlying mechanism was to employ a Schrodinger-Poisson coupled solver. Plus, COMSOL provided many physics interfaces and add-ons right out of the box. Moreover, COMSOL had a myriad of documentation, ranging from blog posts to full-fletched video tutorials. The documentation that came in with the software was highly informative as well. COMSOL also supports integration with various software such as Excel and MATLAB which is referred to as a "Livelink". While searching for existing research done in COMSOL, it was found that simulations and studies have been done to find the depletion-all-around operation of n-channel four gate field effect transistors via the Poisson-Schrodinger equation [9].

Out of all the elegant physics interfaces COMSOL has to offer, we found the Semiconductor interface best suited for our work. Later, we had to integrate the Schrodinger equation via COMSOL's physics builder tools. In the next few sections, some of the features of COMSOL that we found quite helpful for our simulation purposes are discussed.

4.2 COMSOL Model Tree Hierarchy

The COMSOL's model tree is essentially a tidy and organized way to build a model by defining its associated attributes, such as method of solving for the model, results and many more [10]. The model tree for our QWFET simulation is shown below:

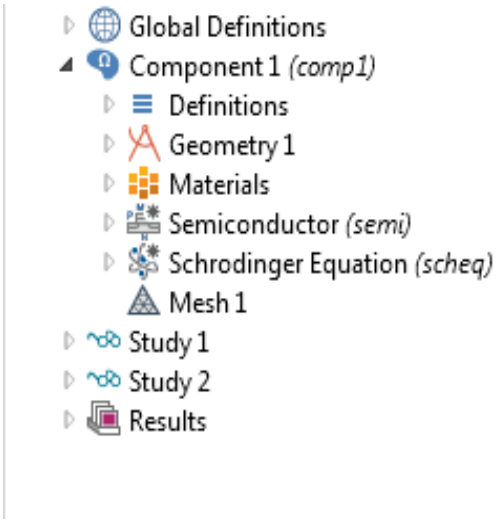

Fig 4.1: The COMSOL Model Tree (Courtesy of COMSOL® Multiphysics®)

The "Global Definition", "Component" and "Study" nodes are the root nodes of our model. Each root node, on accessing, reveals several sub-nodes. For instance, the component node collapses to several sub-nodes, each focusing on a certain aspect of the model, such as the material used in the model, or the type of physics interfaces being implemented in the model. This hierarchical system of information representation in COMSOL proved to be very helpful, since specific information is abstracted neatly into a node or sub-node.

4.3 Materials Library

The materials library is a special COMSOL add-on that comprises of a immense number of material properties, namely in the form of data or piecewise polynomial functions [11]. Since one of our simulation objectives involved changing the material of the upper layer of the QWFET, a large library of materials was one of the reasons COMSOL was chosen. Moreover, if a material of interest is not available, a custom materials library can be easily created or can be imported from an external source. For the purpose of our simulation, we chose Indium Phosphide (InP) and Indium Aluminum Arsenide (InAlAs) as materials from the library. Although all the properties we required for the simulation were not provided by COMSOL, it did provide the option to add more custom parameters.

4.4 The Physics Interfaces

A Physics Interface in COMSOL provides all the domains, boundary conditions and the associated equations required for modeling a physical phenomenon or system. COMSOL also has the option for creating custom Physics interfaces. At the same time, some compatible physics interface can be coupled to one another. The two physics interface that we have used for our simulations – the semiconductor interface and a custom Schrodinger interface.

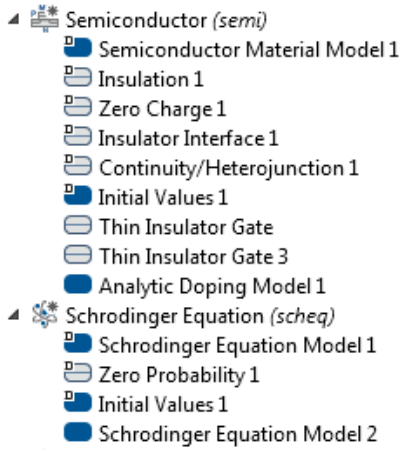

Fig 4.2: The Physics Interfaces (Courtesy of COMSOL® Multiphysics®)

The semiconductor physics interface was created to assist the simulation of semiconductor devices, which is a much feasible and cost effective way rather than actually prototyping the devices. The above diagram illustrates the initial conditions and boundary conditions that were incorporated with our model.

The Schrodinger physics interface was a custom interface that we had to integrate to COMSOL ourselves via the physics builder tool.

4.5 Studies

A typical COMSOL study comprises of a set of solvers that is used for computation. For a particular simulation, a suitable study is chosen in conjunction with the type of physics interface being used. In our simulation setup, the Stationary study was selected as a solver for the Semiconductor interface, while the Eigenvalue study was selected as a solver for Schrodinger interface. The stationary study was chosen since our electrostatics simulation is time-independent, and eigenvalue study was employed to calculate the probability density at each eigenstate.

4.6 Finite Element Method

The Finite Element Method (FEM) is employed by COMSOL behind the scene in order to find approximations to partial differential equations. Almost at all times, a simulation demands the solution of multiple partial differential equations.

In case of FEM, a single equation is approximated by a set of numerical model equations. This concept is better known as “discretization”. Once the equation has a set of numerical components, each can be solved individually via numerical methods, and is then combined to yield the approximate solution to the partial differential equation.

The finite element method can be observed to be employed extensively in the engineering community [12], primarily because of the freedom it provides while creating each element. The

element distribution can be uniform or non-uniform, and hence can be manipulated to provide a required resolution. COMSOL provides multiple options for manipulating the element mesh distribution, ranging from normal to extra-fine to coarse.

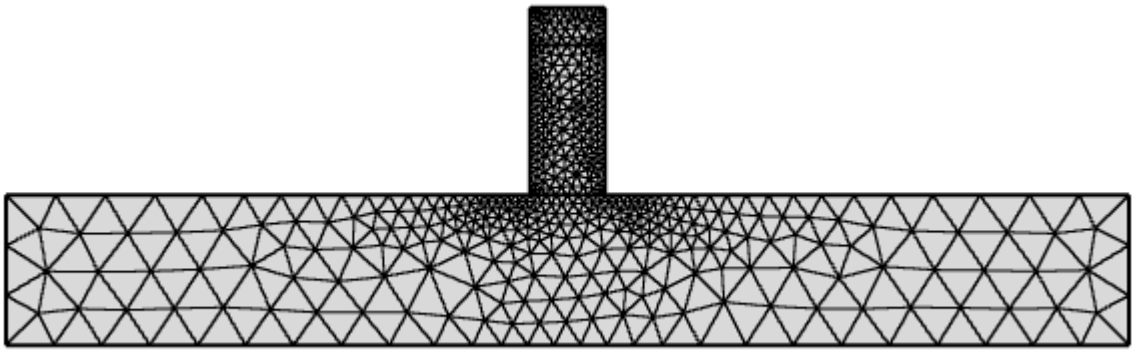

Fig 4.3: Mesh creation by using FEM elements in COMSOL®

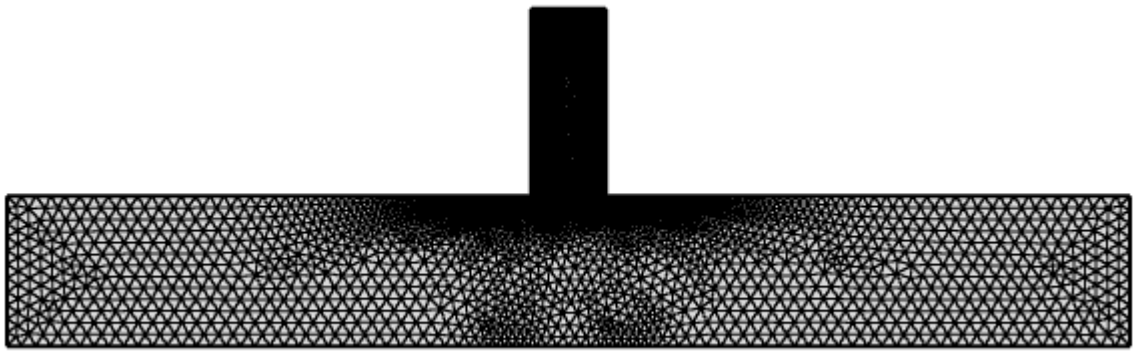

Fig 4.4: Extra fine mesh creation using FEM elements in COMSOL®

5. THE SIMULATION METHODOLGY

5.1 Simulation Process

The primary simulation objective is to essentially derive the CV (Charge vs. Voltage) characteristics for the following scenarios:

a) Two different materials for the upper boundary, namely Indium Phosphide and Indium Aluminum Arsenide.

b) By adding doping to the upper and lower boundary (avoiding the channel).

For each of the above scenarios, the gate voltage is varied from 0 to 1.2 volts with a 0.2-volt interval each time.

The process of obtaining the CV curve for each scenario is almost similar. The entire process is elucidated below:

a) Firstly, appropriate studies and physics interfaces were selected for the simulation via the COMSOL model wizard. For our simulation, the Semiconductor Module with stationary study was selected. The semiconductor module works best for simulated devices up to 100 nanometers. Hence, to explore the semi-classical aspects, the Schrodinger equation was also incorporated via the Physics Builder, along with the eigenvalue study.

b) A geometry of the cross-section of the device is then created via primitive shapes (rectangle and points), and some custom shapes were created via “union”.

c)Next, materials were added to the geometry in the following manner:

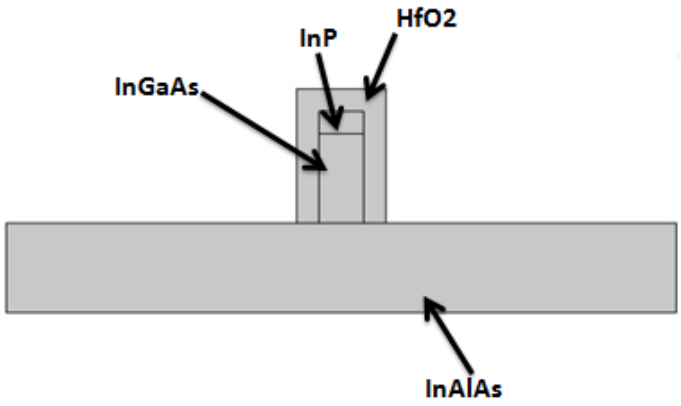

Fig 5.1: Materials applied to different parts of the geometry

d) Next, a "thin insulator gate" boundary was added to the geometry via the Semiconductor module in order to apply gate voltage.

e) After setting the gate voltage to a desired value (start at 0 volts), the stationary study is ran in order to compute with the parameters set forth by the semiconductor module.

f) After convergence is achieved, a cut-line plot is used to plot the conduction band profile vertically across the device:

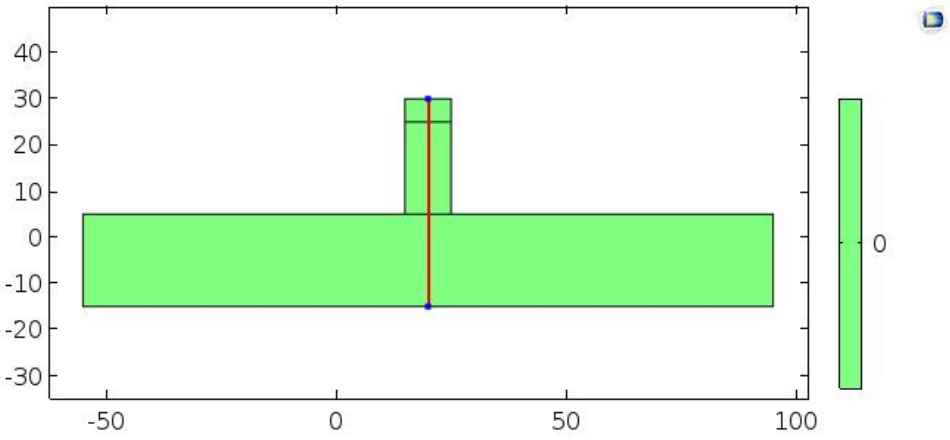

Fig 5.2: A vertical cutline for conduction band

g) Using the data from the conduction band plot, an interpolated function for the conduction band is generated. This is then fed as the potential energy to the Schrodinger interface. This action initiates the pseudo-coupling of the two physics interfaces. Note that, this coupling is being referred to as "pseudo", since this is not an idea Schrodinger-Poisson solver.

h) The eigenvalue study is then set to compute, which initiates the Schrodinger physics interface. After convergence, the probability plot density data is fed to a MATLAB code via MATLAB LiveLink.

5.2 1D Fermi Dirac Function implementation in MATLAB

The one dimensional Fermi-Dirac function is derived from [13]. This was coded in MATLAB so that kinetic energy of the system becomes incorporated with the potential energy as a whole.

$$\therefore F(E) = \frac{1}{1 + e^{E - E_F / K_B T}}$$

But due to the effect of k-space (considering a 1-D k-space), the Fermi-Dirac distribution had to be integrated in the k-space. The equation becomes:

$$F^*(x) = \frac{1}{L}\sum_{k_x} f_0\left(E + \frac{\hbar^2}{2m_c}({k_x}^2)\right)$$

$$= \int_0^{\infty} \frac{dk}{2\pi}\left[\frac{1}{1+(e^{E_c/k_B T}.e^{\hbar^2 k^2/2m_c k_B T})}\right] \qquad \text{------eq}^{\text{n}}\text{(i)}$$

Again,

$$y = \frac{\hbar^2 k^2}{2m_c k_B T}$$

$$\Rightarrow \frac{dy}{dk} = \frac{2\hbar^2 k}{2m_c k_B T} \qquad \text{-----eq}^{n}\text{(ii)}$$

Putting,

$$k^2 = \frac{2m_c k_B T y}{\hbar^2}$$

$$\Rightarrow k = \frac{\sqrt{2m_c k_B T}.\sqrt{y}}{\hbar}$$

in eq^{n}(ii), we get:

$$\Rightarrow dk = \frac{\sqrt{2m_c k_B T}}{2\hbar\sqrt{y}}\, dy$$

Again putting the value of dk in eq^{n}(i):

$$F^*(x) = \frac{\sqrt{\sqrt{2m_c k_B T}}}{4\pi\hbar}.\int_0^\infty \frac{1/\sqrt{y}}{1 + e^{(y+x)}}\, dy$$

6. THE MAIN INFERENTIAL OBJECTIVES

a) Experimenting with upper barrier as InP and then as InAlAs.

b) Incorporation of P-Type Doping.

c) Observation of Conduction Band Energy Levels and corresponding probability densities of electrons.

d) Changing Gate Voltages.

e) Finally deducing the gate capacitance and gate voltage characteristics.

List of Materials Used and Their Properties:

Material	Relative Permittivity	Band Gap (V)	Electron Affinity (V)	Effective Density Of States, Valence Band ($1/cm^3$)	Effective Density Of States, Conduction Band ($1/cm^3$)	Electron Mobility ($cm^2/V.s$)	Hole Mobility ($c\,m^2/V.s$)
HfO2	25	5.5	4.05	1.04e19	2.8e19	10	12
$In_xAl_{1-x}As$	12.44	1.46	4.4	1.11e19	1.49e15	8800	220
InP	12.5	1.344	4.38	2.2e15	1.1e14	5400	200
$In_{1-x}Ga_xAs$	14.2	0.74	4.5	1.05e15	4e13	12939	300

Table 1: Various properties of materials used

The various parameters of some materials, **not** being present in COMSOL® Multiphysics®, were calculated as follows [14]:

$In_{1-x}Ga_xAs$ Parameters, for x=0.47:

1. Band Gap(eV)=

$$(\mathbf{0.36 + 0.63x + 0.43x^2})$$

2. Electron Affinity(eV)=

$$(\mathbf{4.9 - 0.83x})$$

3. Effective Density of States, Valence Band $(1/cm\text{^}3)$=

$$\mathbf{4.82\ x\ 1015\ x(0.023 + 0.037x + 0.003x2)\text{^}(\frac{3}{2}) * \ T\text{^}(\frac{3}{2})}$$

4. Effective Density Of States, Conduction Band $(1/cm\text{^}3)$ =

$$\mathbf{4.82\ x\ 1015\ x\ (0.41 - 0.1x)^{\frac{3}{2}} * \ T\text{^}(\frac{3}{2})}$$

5. Electron Mobility$(c\ m^2/V.s)$=

$$(\mathbf{40 - 80.7x + 49.2x^2})$$

6. Hole Mobility$(c\ m^2/V.s)$= **300** (For T=300K)

The parameters for $In_xAl_{1-x}As$ was calculated from [13].

7. INFERENCES ON QWFET WITH InP AS UPPER BARRIER

7.1 At Vg = 0V

We have obtained the following results:

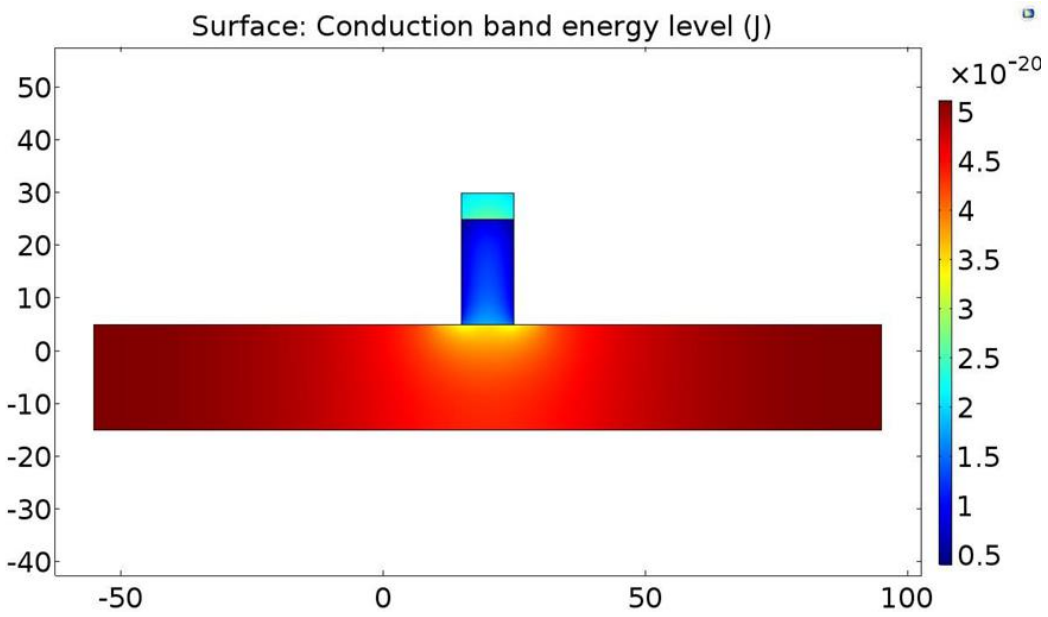

Fig 7.1.1: Conduction Band Profile with no doping

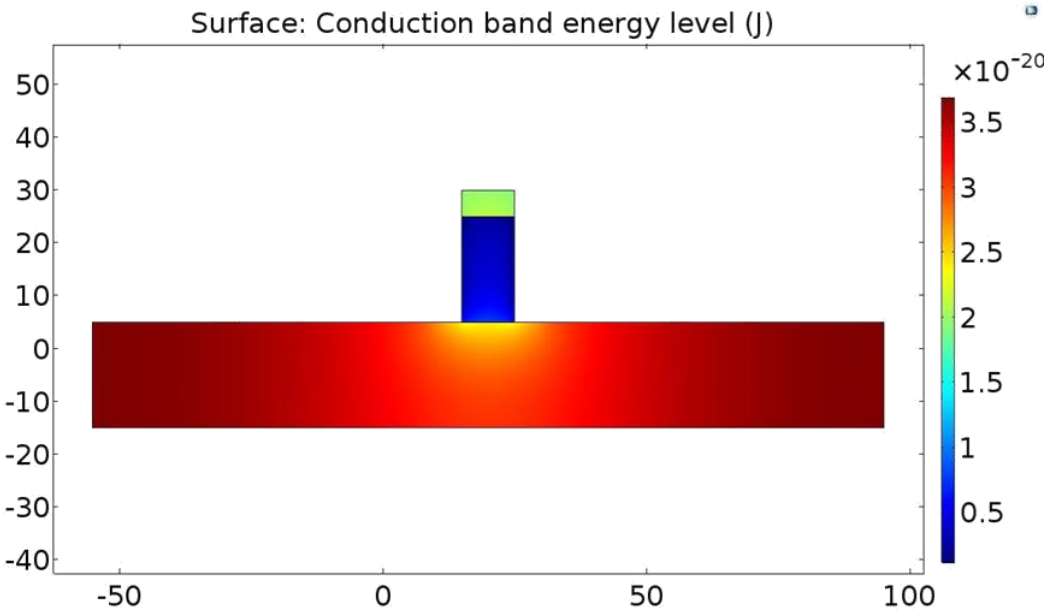

Fig 7.1.2: Conduction Band Profile with p-type doping

From the above figures we can see that there is a significant drop in the conduction band energy profile throughout the entire geometry after p-type doping is applied to the upper and bottom barriers. This happens as the effective fermi level goes down due to the excessive p-type holes [16].

More inferences on this matter are as follows:

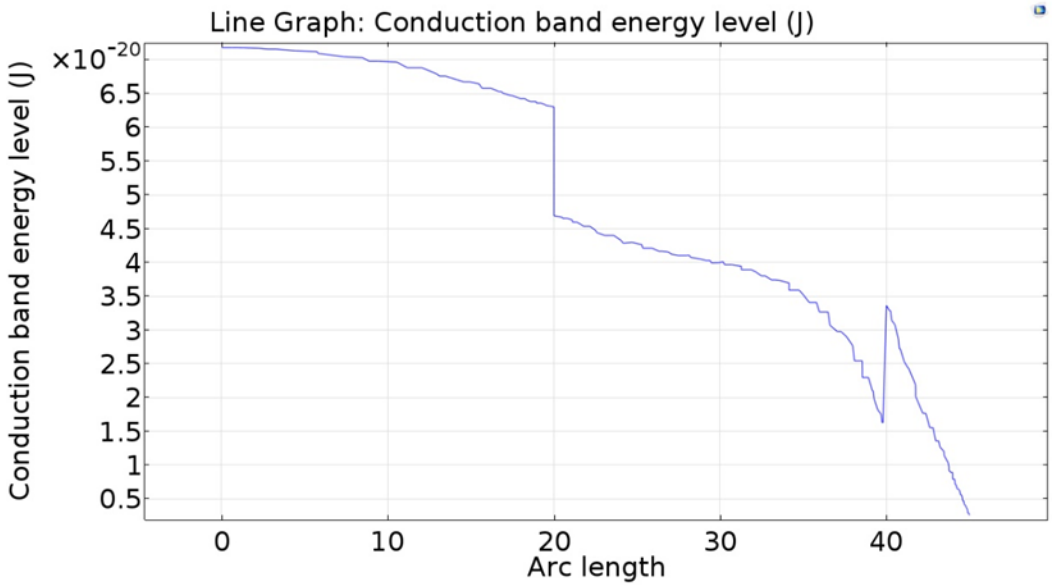

Fig 7.1.3: Conduction Band Energy Level with no doping

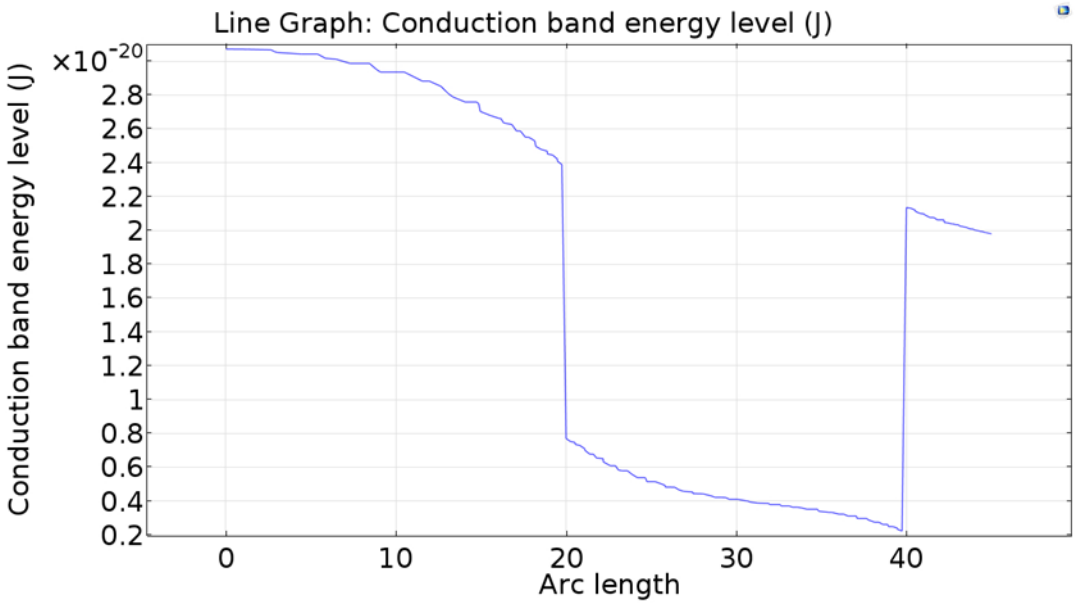

Fig 7.1.4: Conduction Band Energy Level with p-type doping

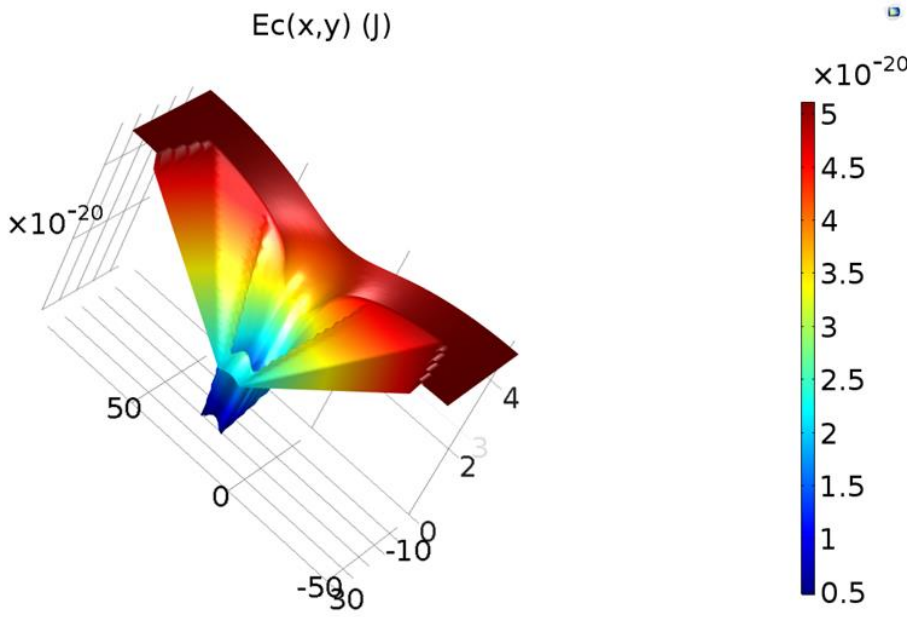

Fig 7.1.5: 3D representation of the Conduction Band Energy Level with no doping

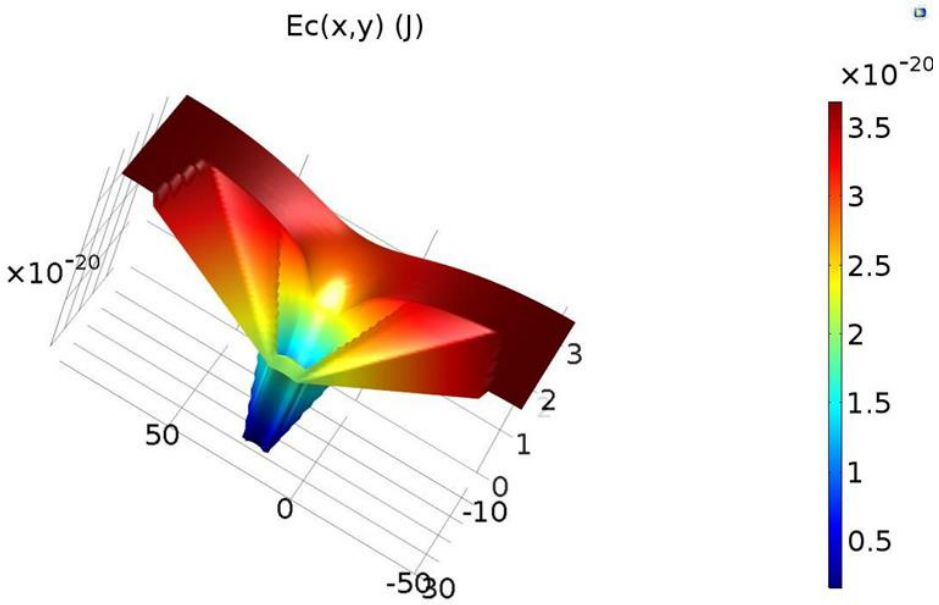

Fig 7.1.6: 3D representation of the Conduction Band Energy Level with p-type doping

From the figures 7.1.5 and 7.1.6 above, we can see that the well-formed is much more prominent when p-type doping is applied to the upper and bottom barriers, hence increasing the 'tunneling effect'. There is also a change of pattern of conduction band energy level from figures 7.1.3 to 7.1.4.

Now putting these conduction band energy levels to Schrodinger's equation, we get the following patterns of probability density throughout the geometry:

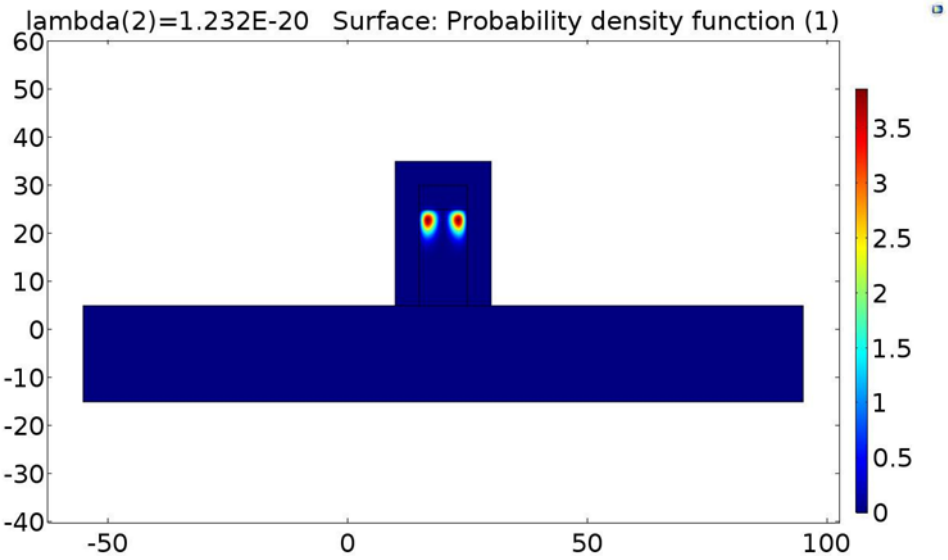

Fig 7.1.7: Probability Density of electrons with no doping

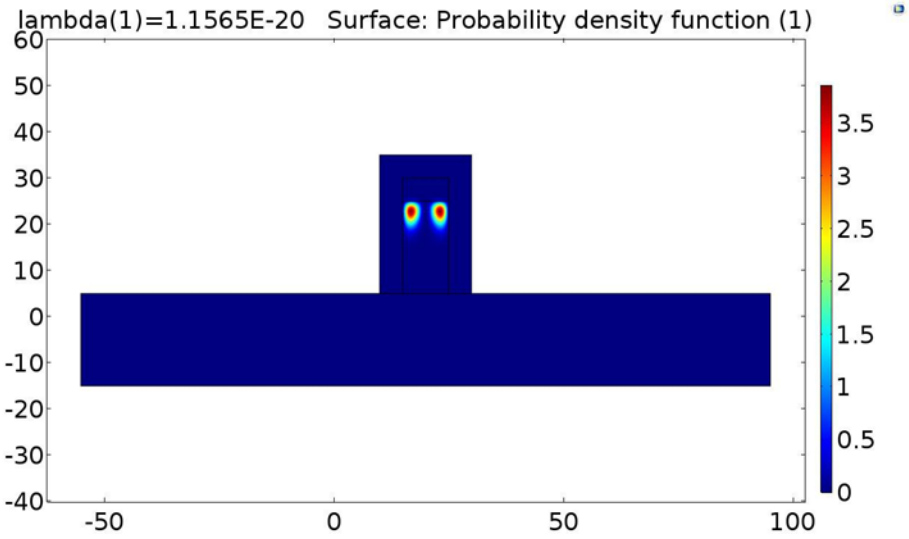

Fig 7.1.8: Probability Density of electrons with p-type doping

So the above probability densities show that there is almost no difference between the doped and undoped conditions when it comes to the likelihood of trapped electron patterns.

Now we will repeat the entire process above by changing gate voltages.

7.2 At Vg = 0.2V

We have obtained the following results:

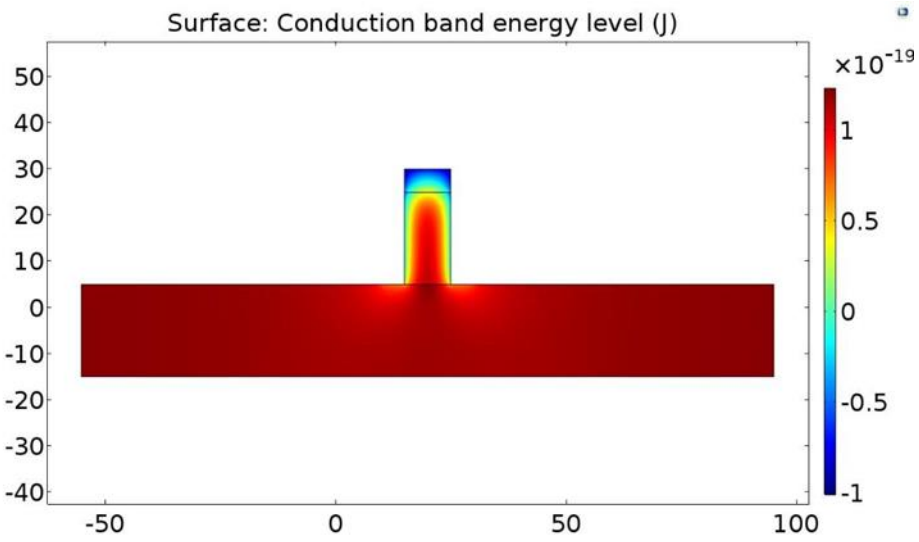

Fig 7.2.1: Conduction Band Profile with no doping

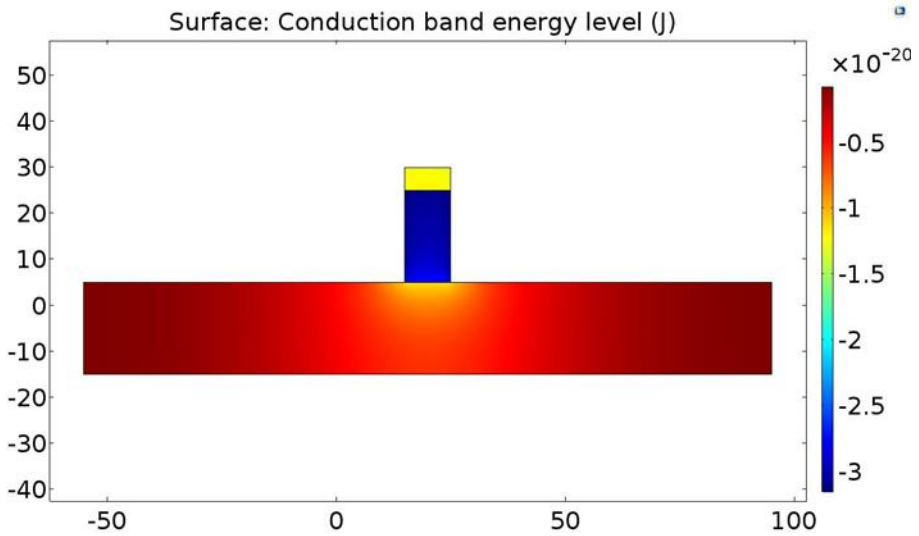

Fig 7.2.2: Conduction Band Profile with p-type doping

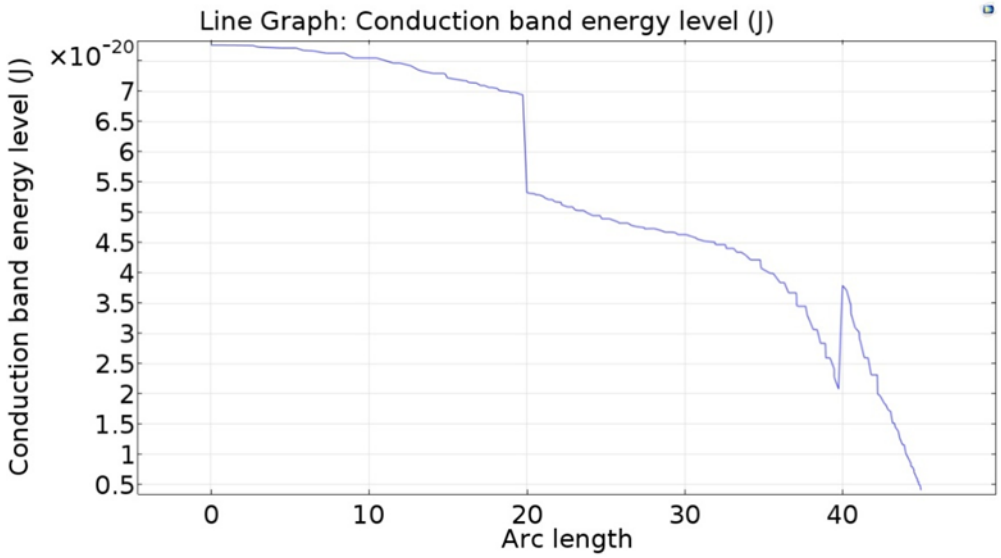

Fig 7.2.3: Conduction Band Energy Level with no doping

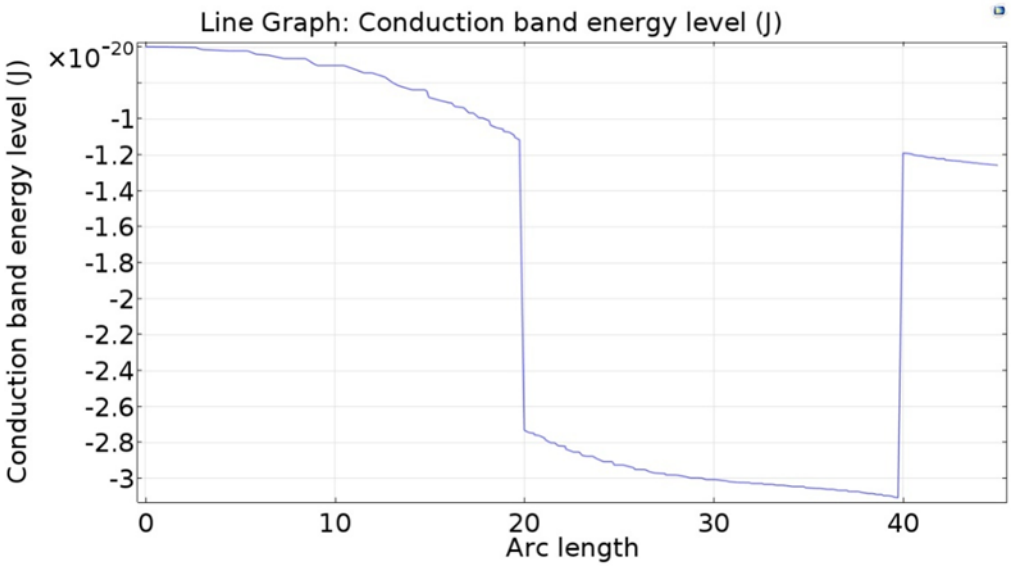

Fig 7.2.4: Conduction Band Energy Level with p-type doping

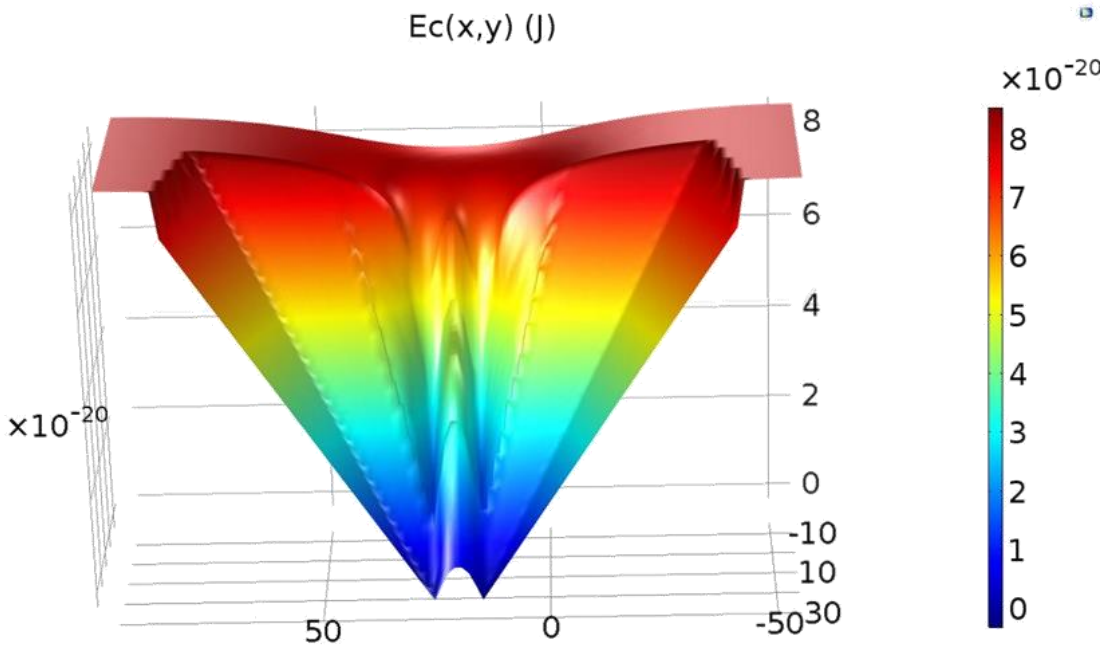

Fig 7.2.5: 3D representation of the Conduction Band Energy Level with no doping

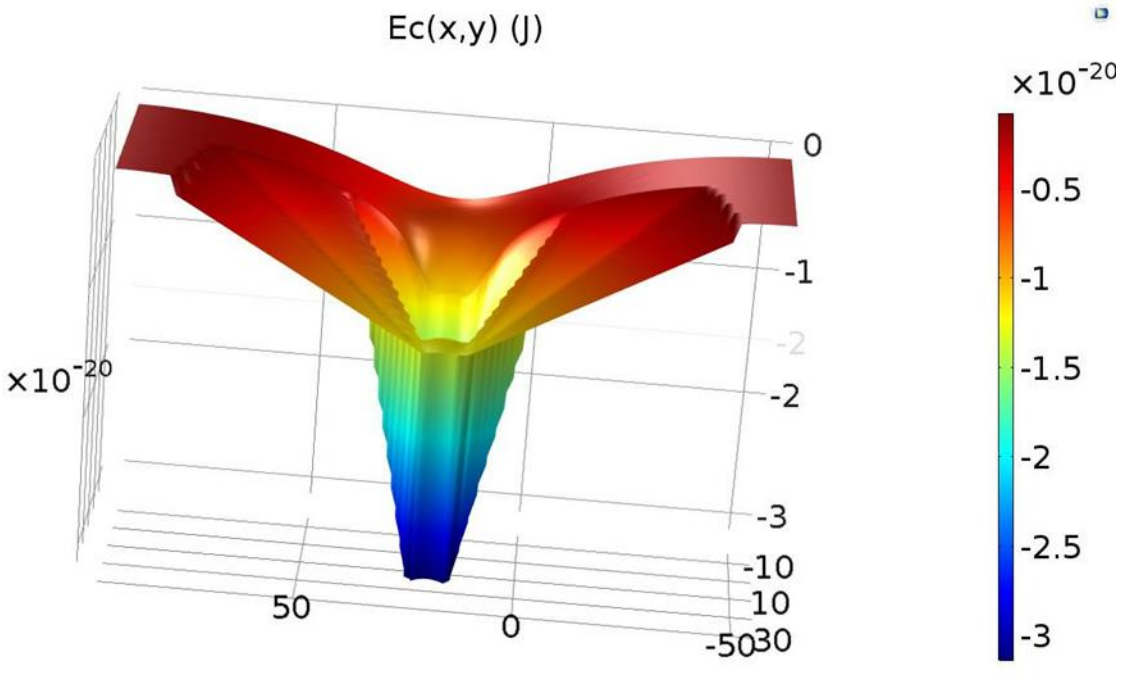

Fig 7.2.6: 3D representation of the Conduction Band Energy Level with p-type doping

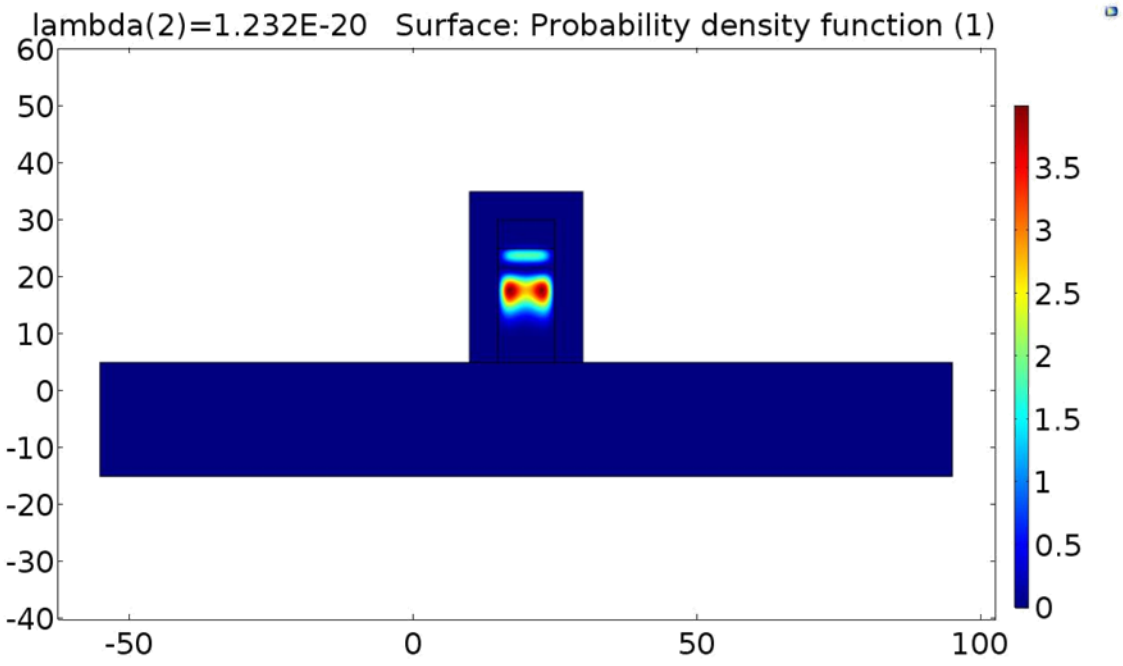

Fig 7.2.7: Probability Density of electrons with no doping

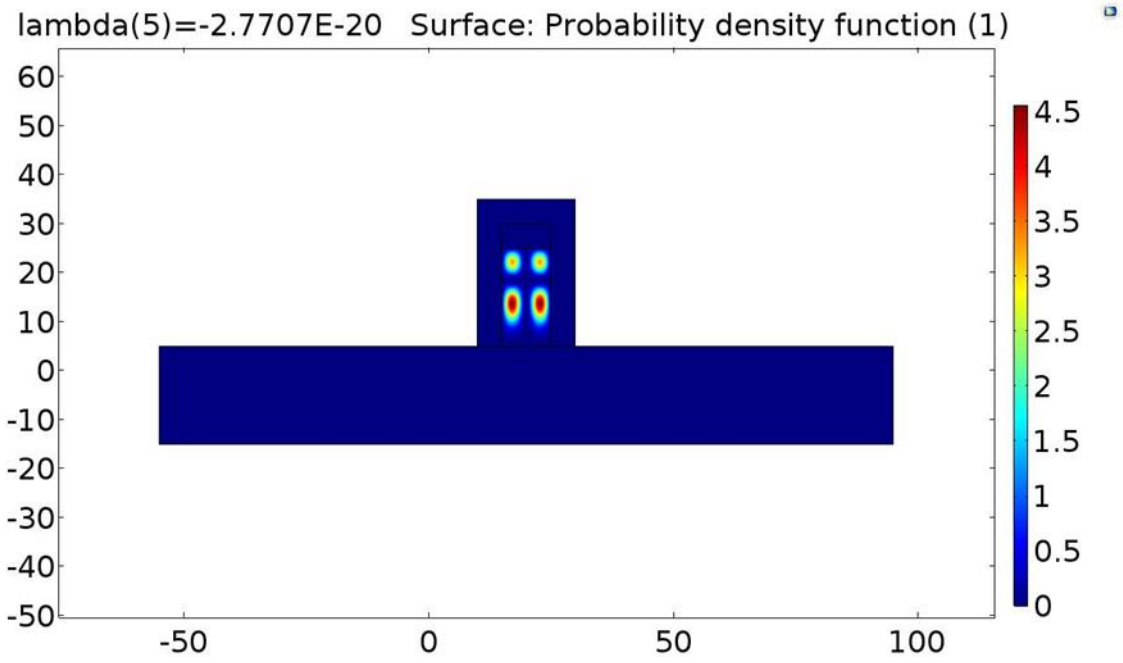

Fig 7.2.8: Probability Density of electrons with p-type doping

From the above set of results, we get the following inferences:

a) From Figures 7.2.1 and 7.2.2, we can see similar results as before as the conduction band energy level decreases across the geometry as p-type doping is implemented.

b) From Figures 7.2.3 to 7.2.4, there is a change in the pattern of the conduction band energy levels.

c) From Figures 7.2.5 to 7.2.6, we can see that the well has again become more prominent.

d) And finally we see that this time with 0.2V Vg applied, the probability density of electrons has now increased quite significantly.

Now we will increase the gate voltage Vg to higher values and see the results.

7.3 At Vg = 1V

We have obtained the following results:

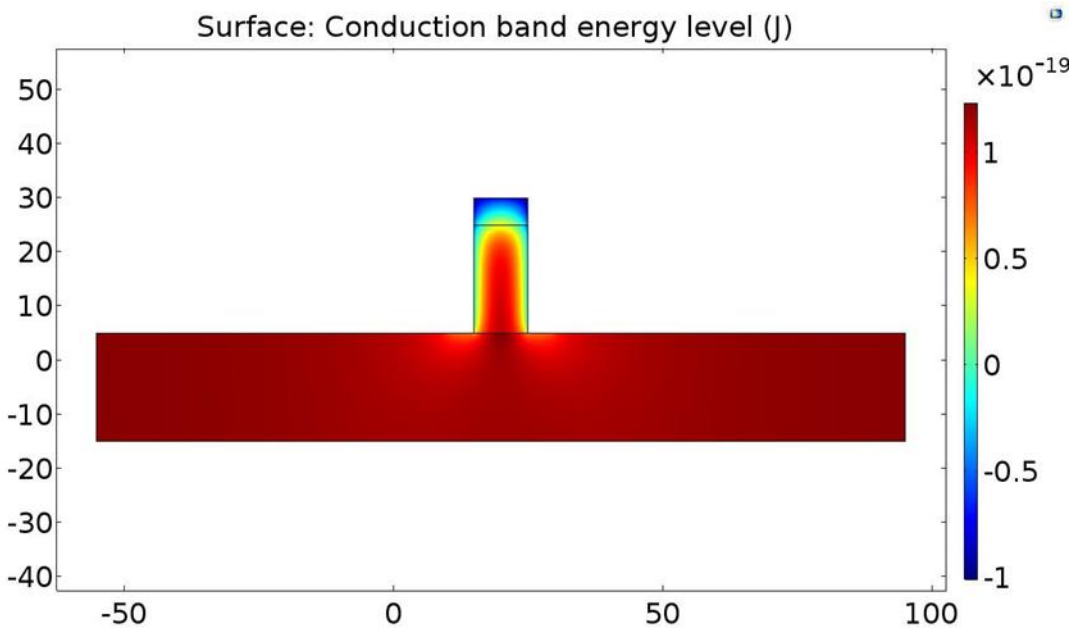

Fig 7.3.1: Conduction Band Profile with no doping

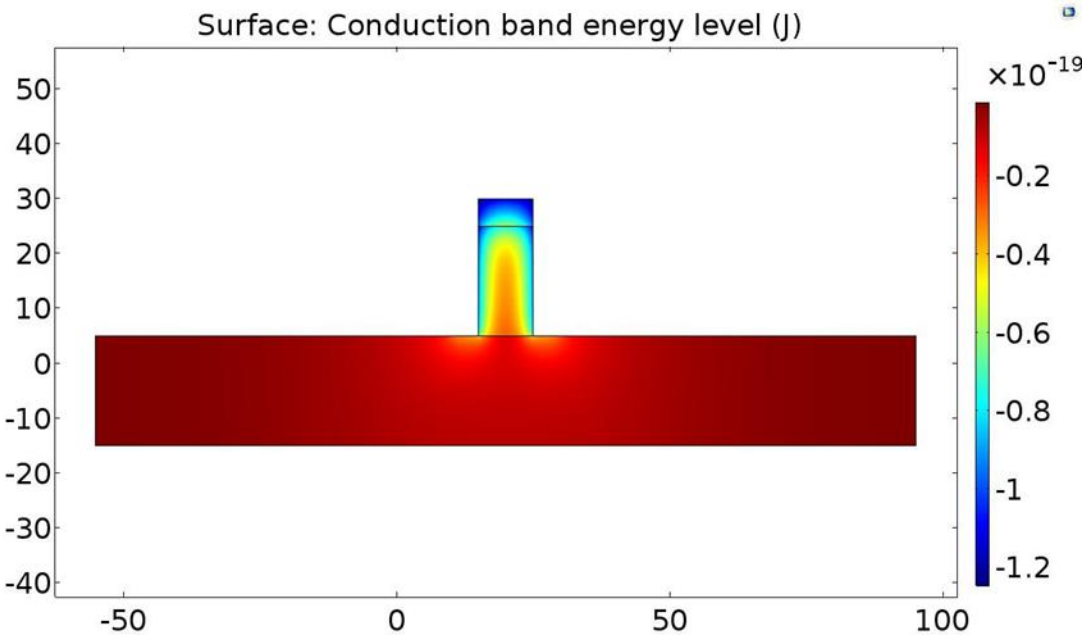

Fig 7.3.2: Conduction Band Profile with p-type doping

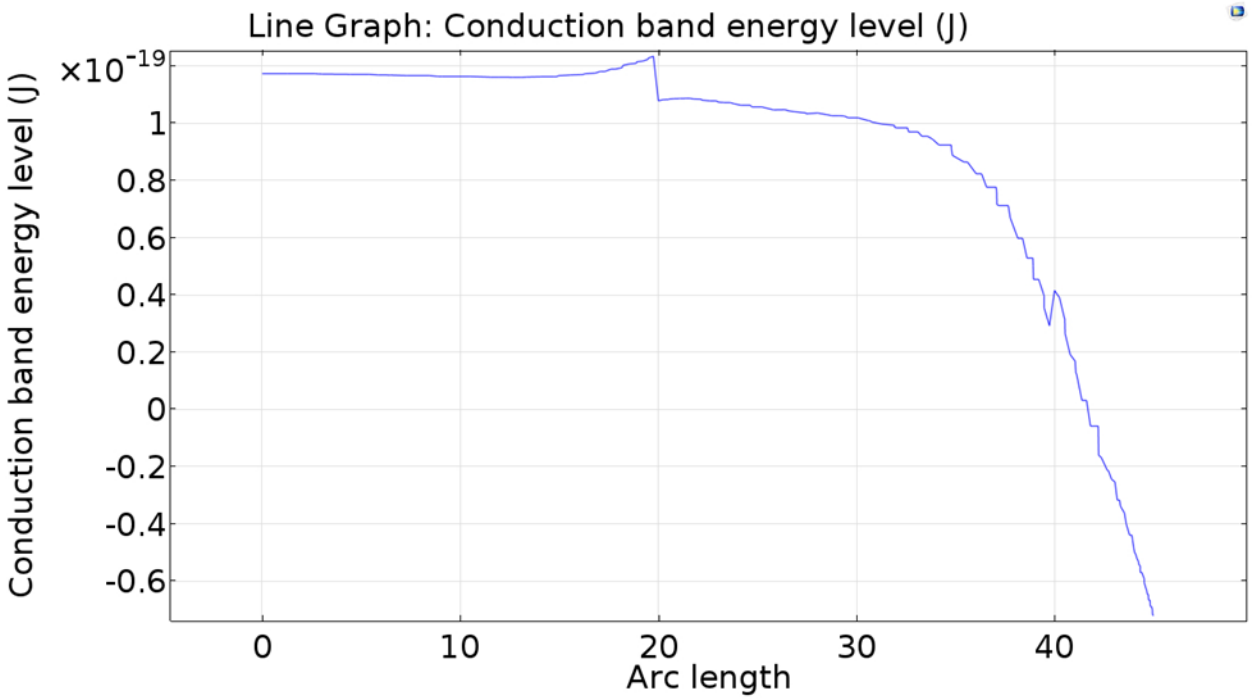

Fig 7.3.3: Conduction Band Energy Level with no doping

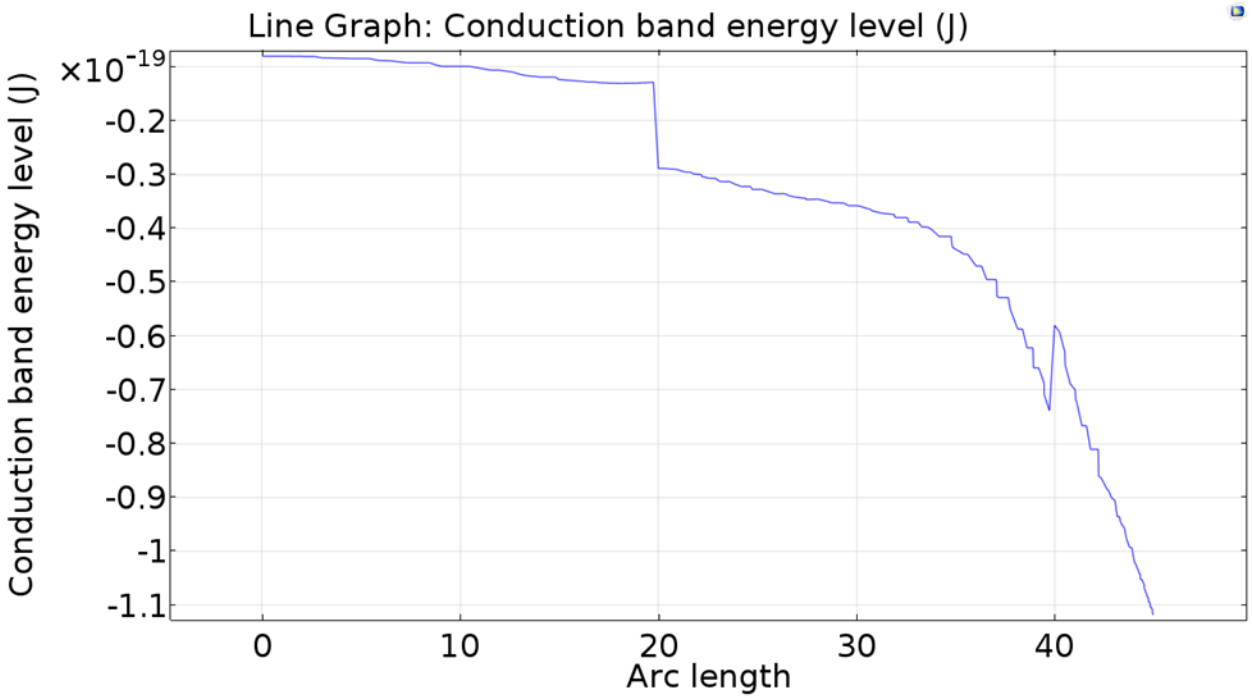

Fig 7.3.4: Conduction Band Energy Level with p-type doping

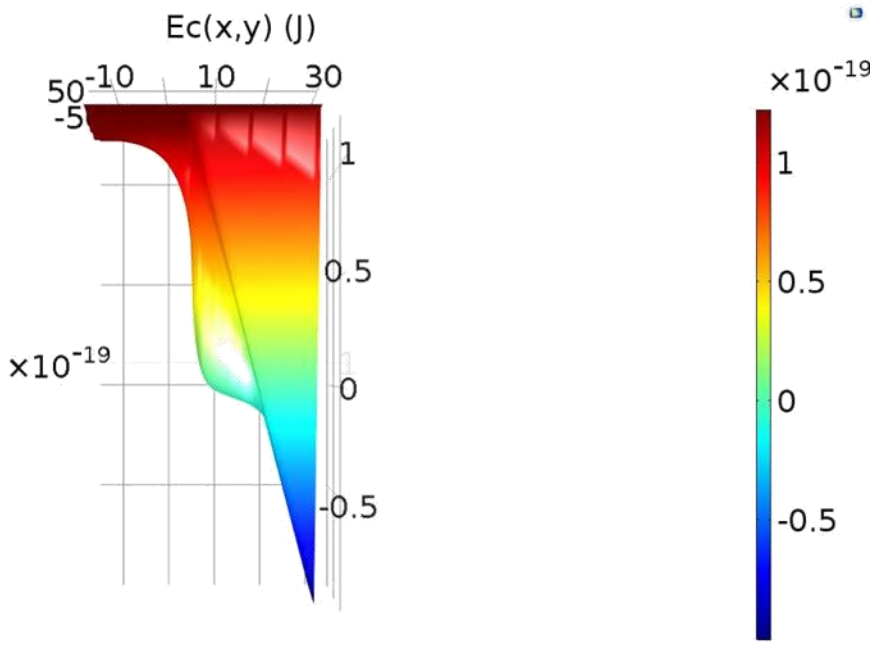

Fig 7.3.5: 3D representation of the Conduction Band Energy Level with no doping

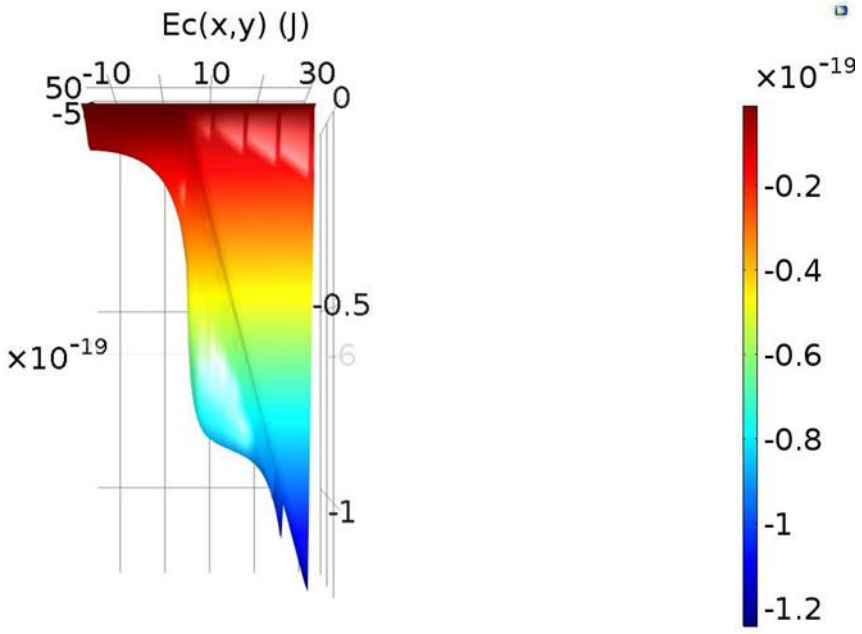

Fig 7.3.6: 3D representation of the Conduction Band Energy Level with p-type doping

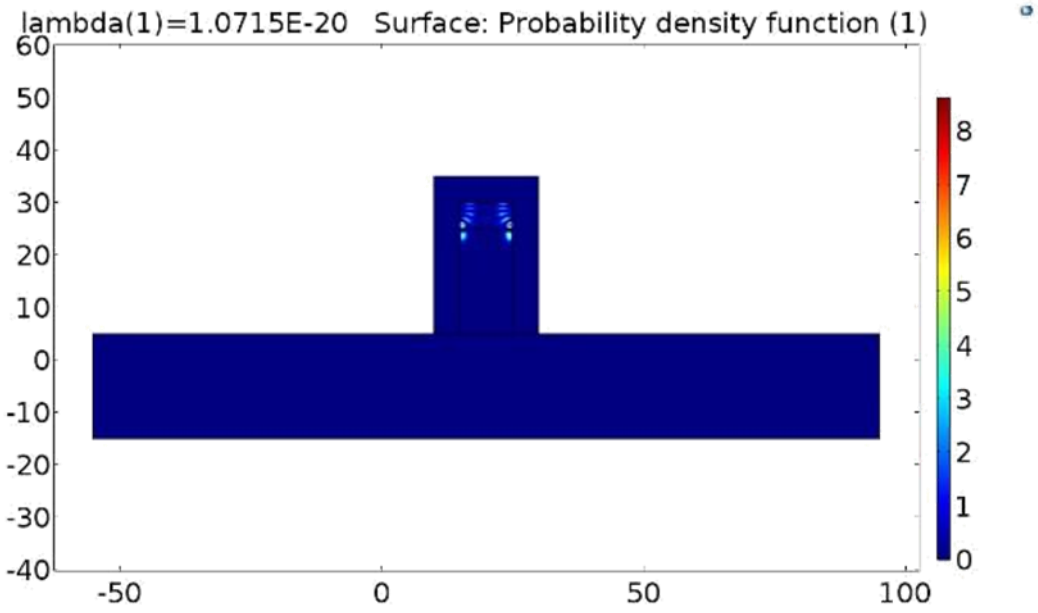

Fig 7.3.7: Probability Density of electrons with no doping

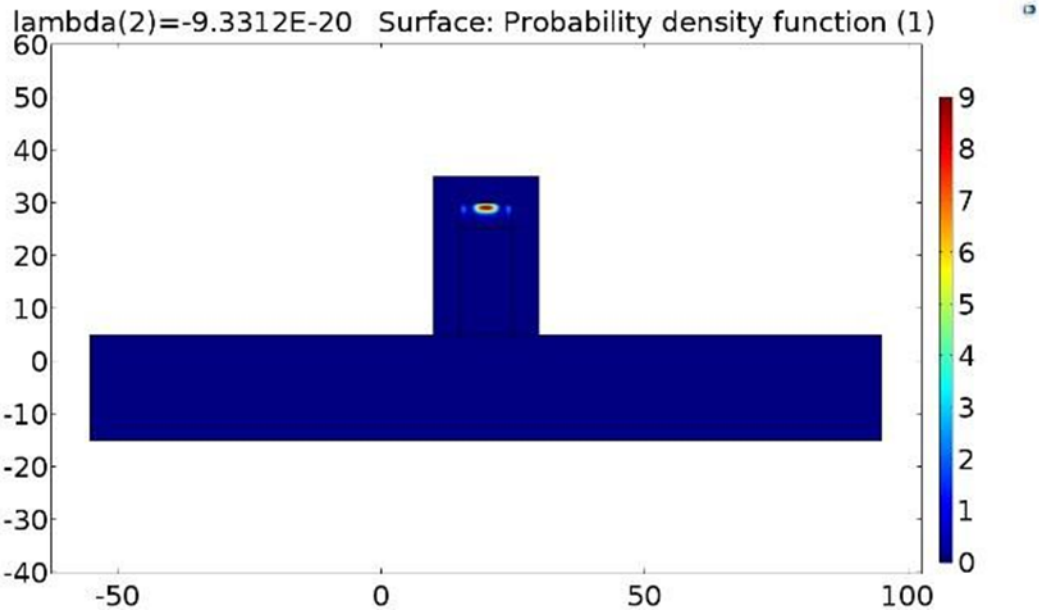

Fig 7.3.8: Probability Density of electrons with p-type doping

From the above figures, we can infer that increasing the voltage yields similar results but with diminishing change.

Now we take our probability densities for different gate voltages and find the charge density in MATLAB. After differentiating our charge density with respect to gate voltage, we have the following results for the with InP as upper barrier:

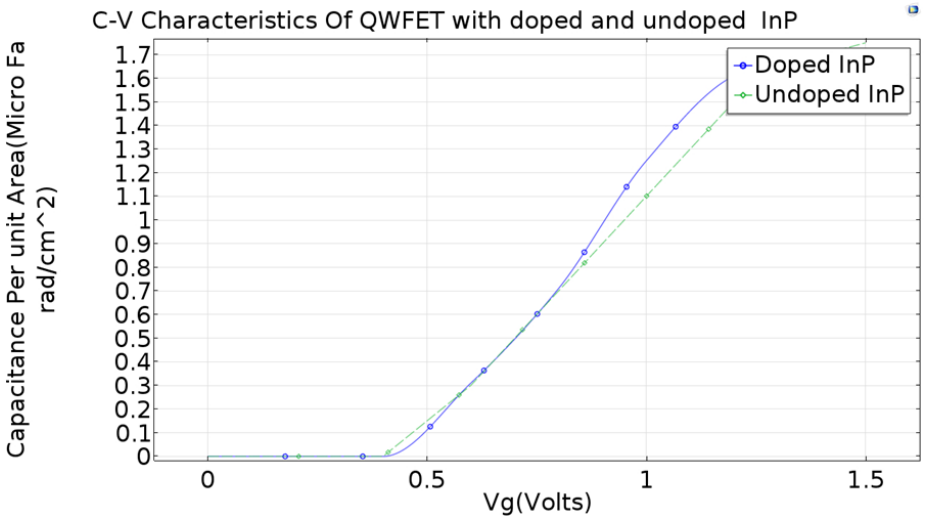

Fig 7.3.9: Comparison of C-V characteristics of QWFET with doped and undoped InP

Our results are consistent with that of Intel Corp. [15]

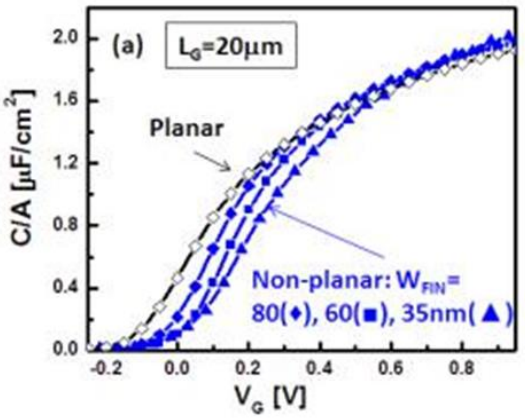

Fig 7.3.10: C-V characteristics with InP by INTEL Corp.

Now that we've inferred about QWFETs with InP as upper barrier, we will now change the upper barrier to InAlAs and perform similar experiments.

8. INFERENCES ON QWFET WITH InAlAs AS UPPER BARRIER

8.1 At Vg = 0V

We have obtained the following results:

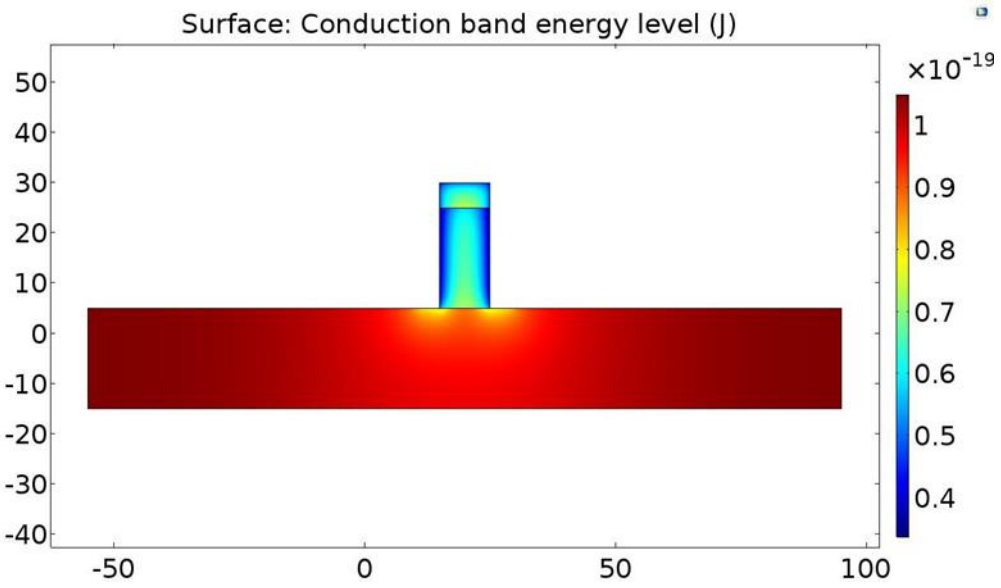

Fig 8.1.1: Conduction Band Profile with no doping

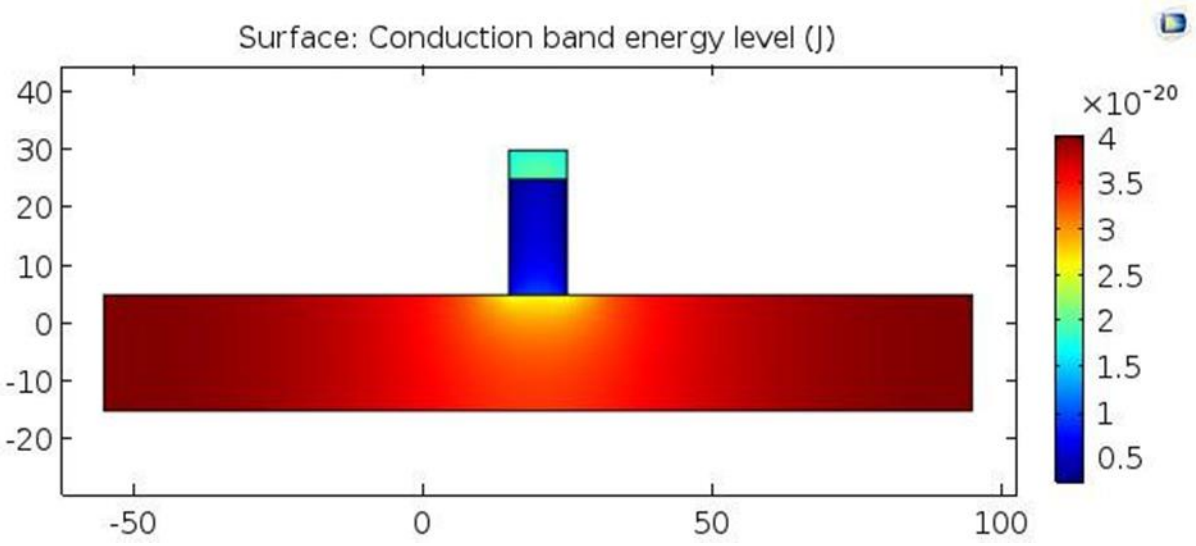

Fig 8.1.2: Conduction Band Profile with p-type doping

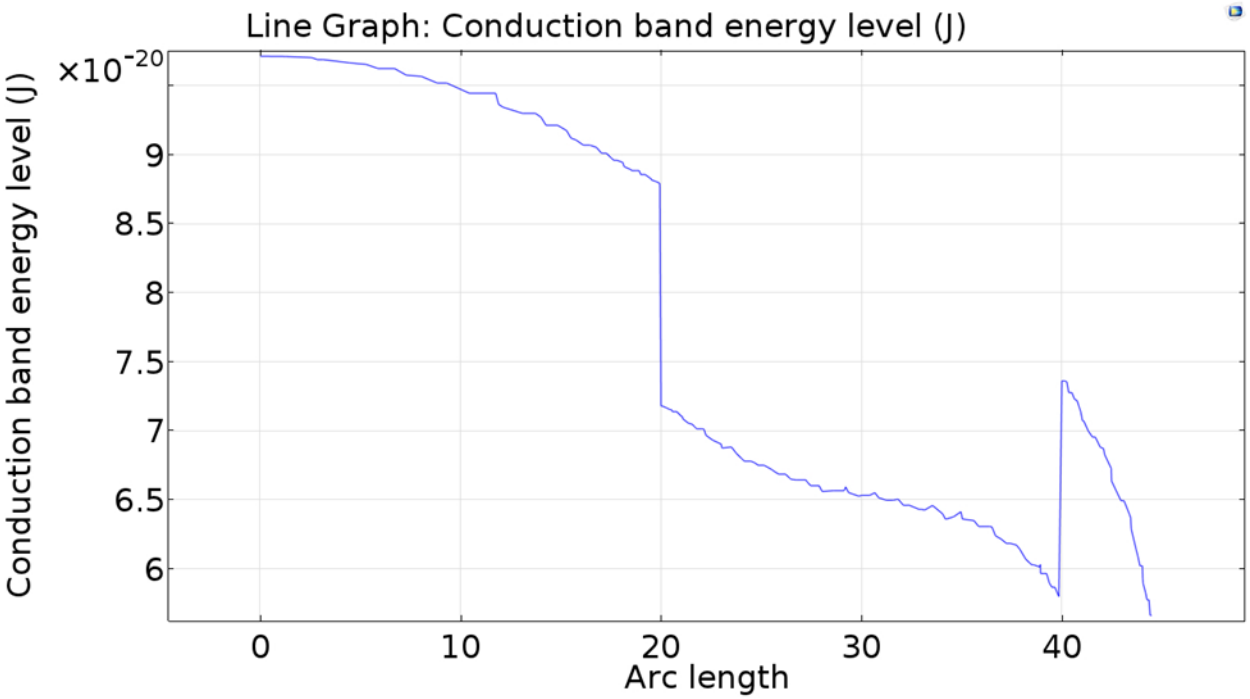

Fig 8.1.3: Conduction Band Energy Level with no doping

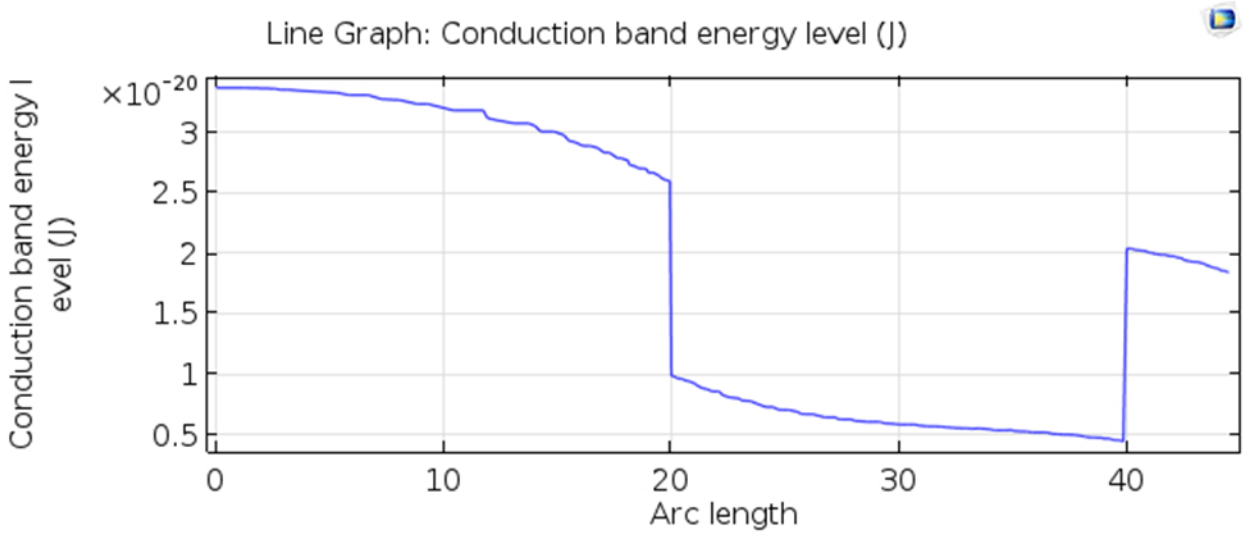

Fig 8.1.4: Conduction Band Energy Level with p-type doping

The preceding figures show that the QWFET with InAlAs as upper layer behaves almost the same as when InP was used. So we now increase the gate voltage and see the results.

8.2 At Vg = 1V

We have obtained the following results:

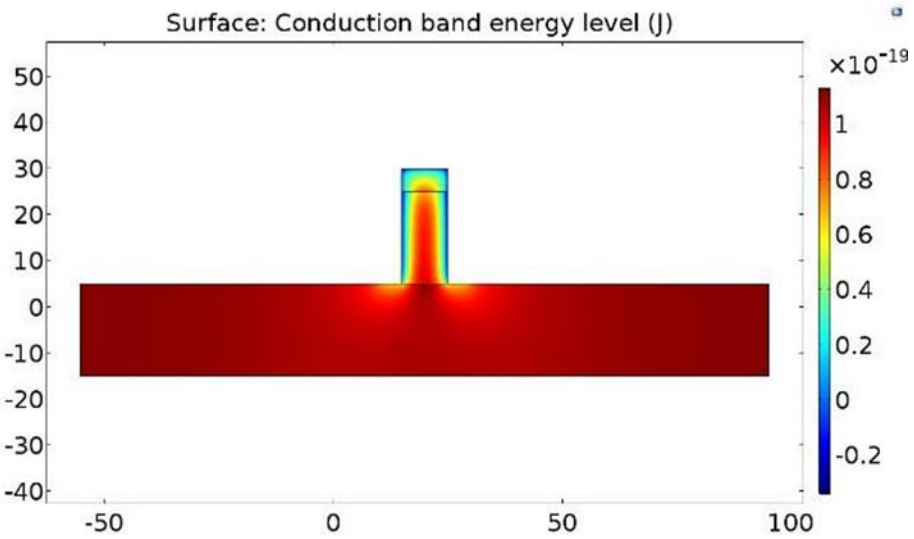

Fig 8.2.1: Conduction Band Profile with no doping

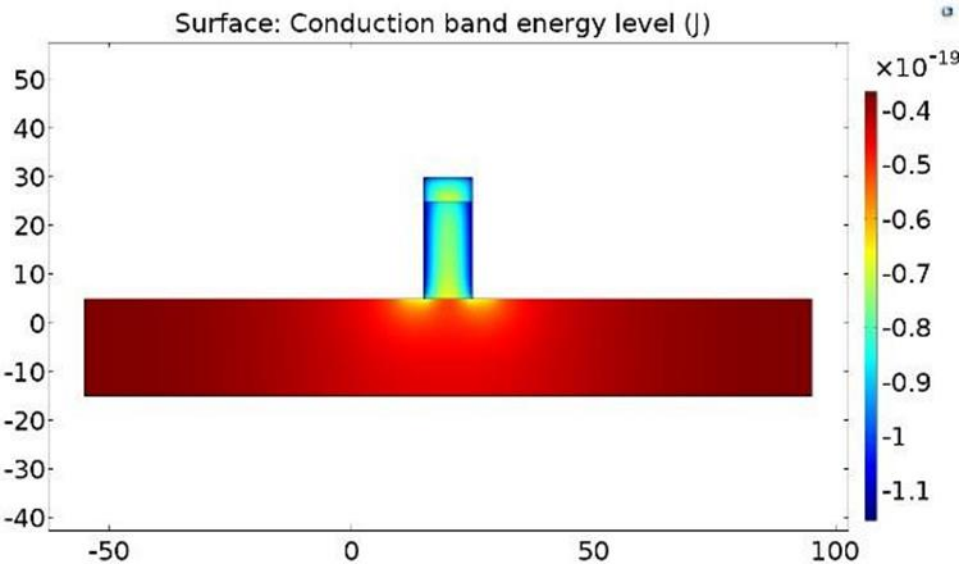

Fig 8.2.2: Conduction Band Profile with p-type doping

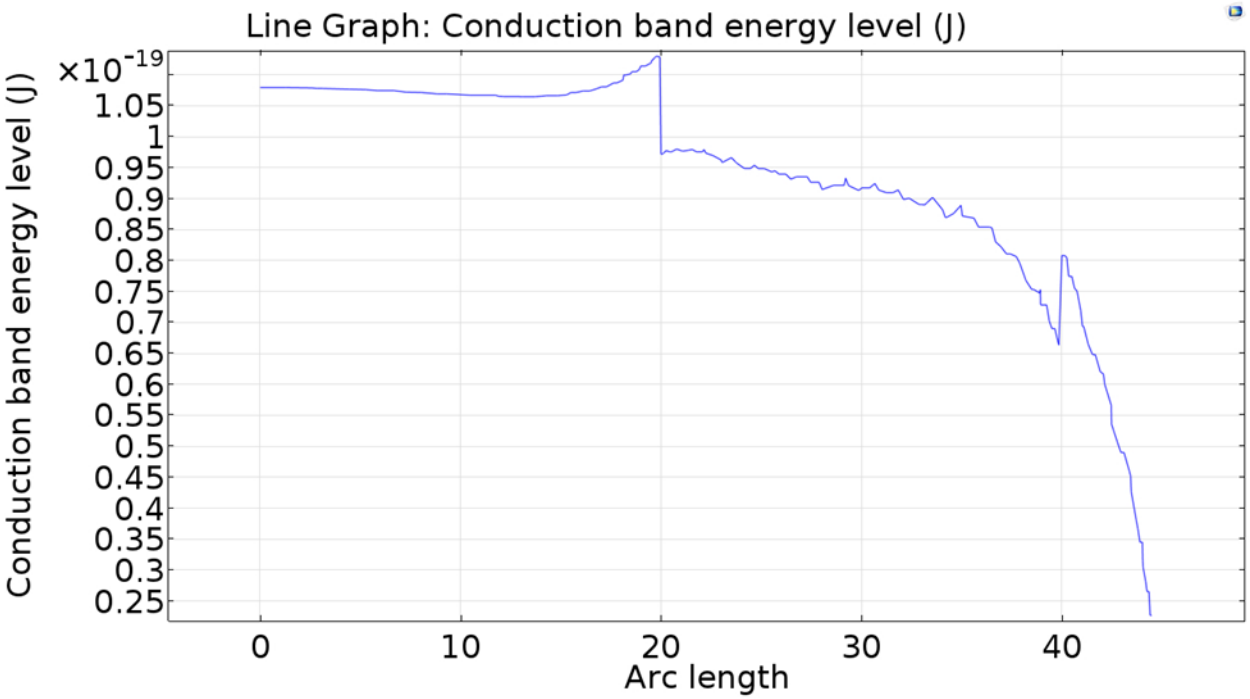

Fig 8.2.3: Conduction Band Energy Level with no doping

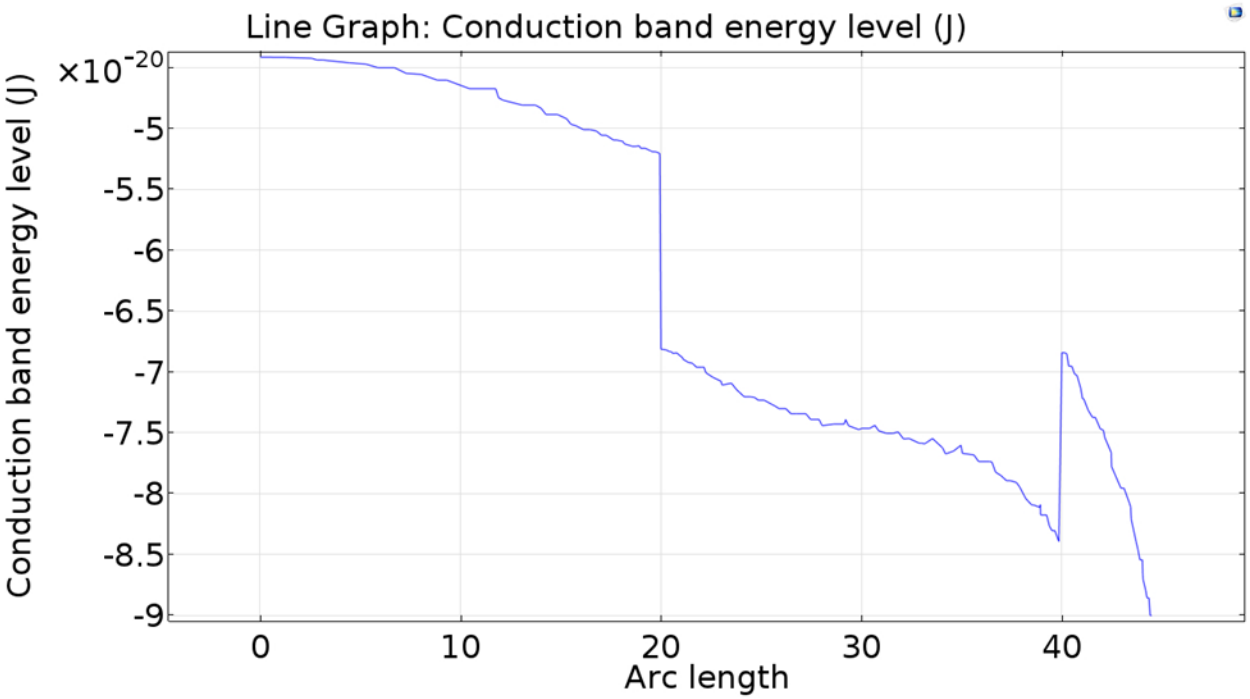

Fig 8.2.4: Conduction Band Energy Level with p-type doping

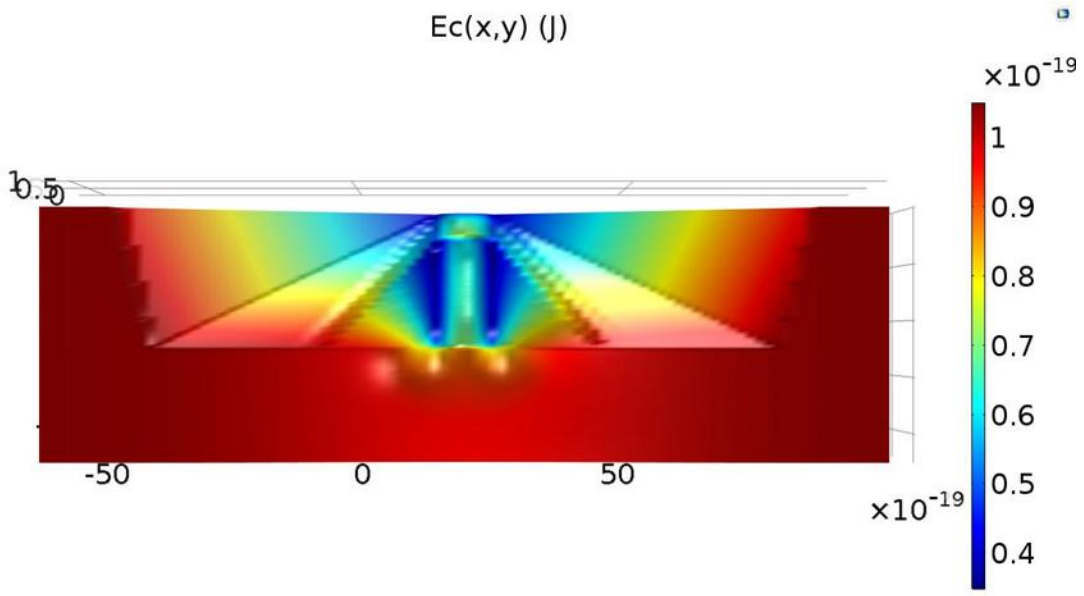

Fig 8.2.5: 3D representation of the Conduction Band Energy Level with no doping

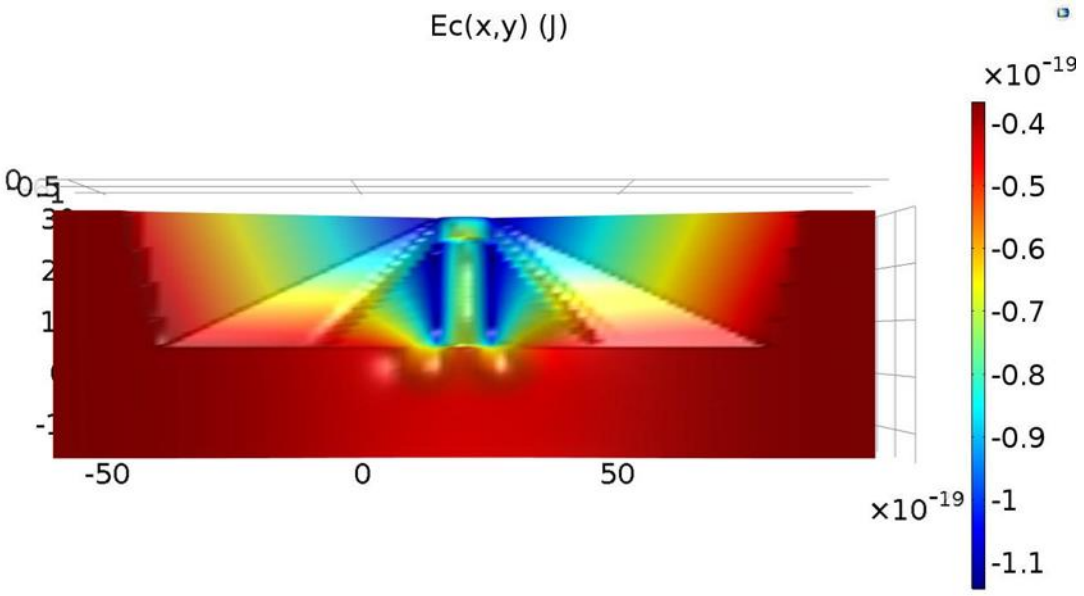

Fig 8.2.6: 3D representation of the Conduction Band Energy Level with p-type doping

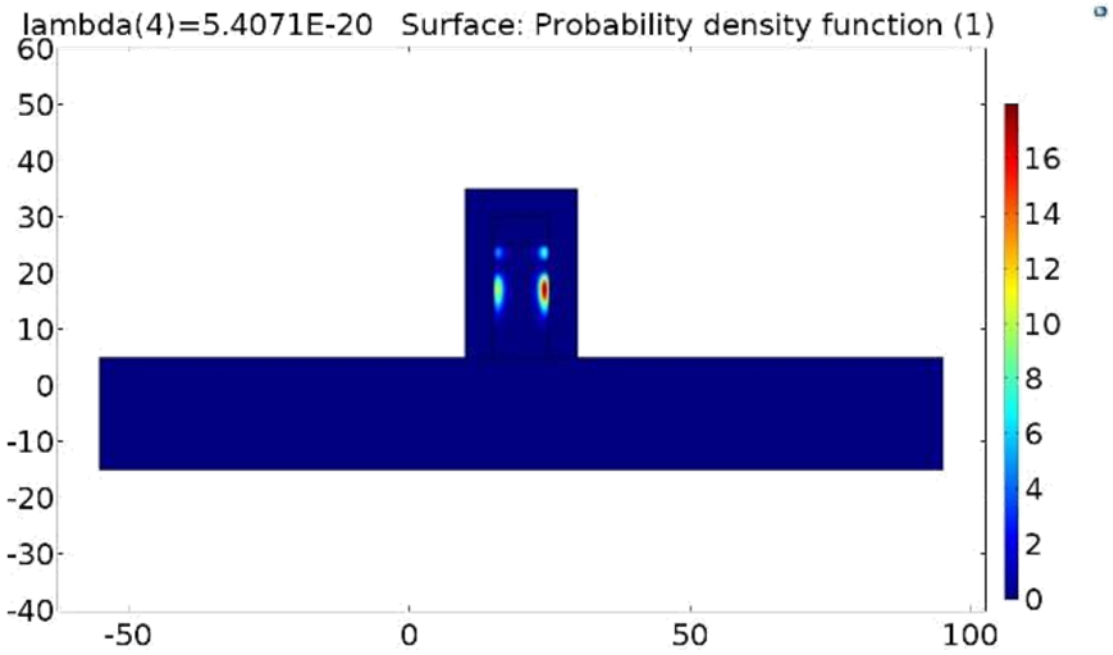

Fig 8.2.7: Probability Density of electrons with no doping

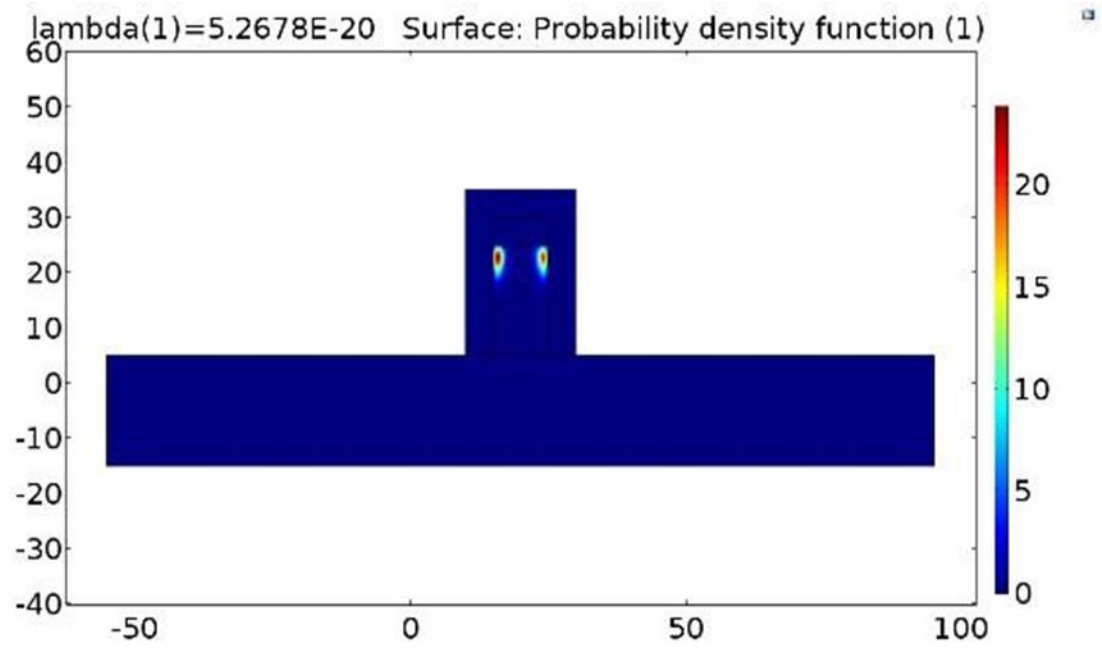

Fig 8.2.8: Probability Density of electrons with p-type doping

From the above diagram, we can infer that the device with InAlAs as upper barrier acts similarly as when InP was used. Few of these inferences are:

a) From Figures 8.2.1 and 8.2.2, we see that as Vg is increased, the conduction band energy level decreases for doped conditions.

b) From Figures 8.2.3 and 8.2.4, we can infer that there is similar but a greater change in the shape of the conduction band energy level than it was with InP.

c) Finally, we can see that while using InAlAs as the upper barrier, the yield of the probability density is much higher for both doped and undoped conditions at higher voltages as compared to when InP was used.

Now we take our probability densities for different gate voltages similarly and find the charge density in MATLAB and we get the charge density similarly by differentiating with respect to gate voltage (V_g):

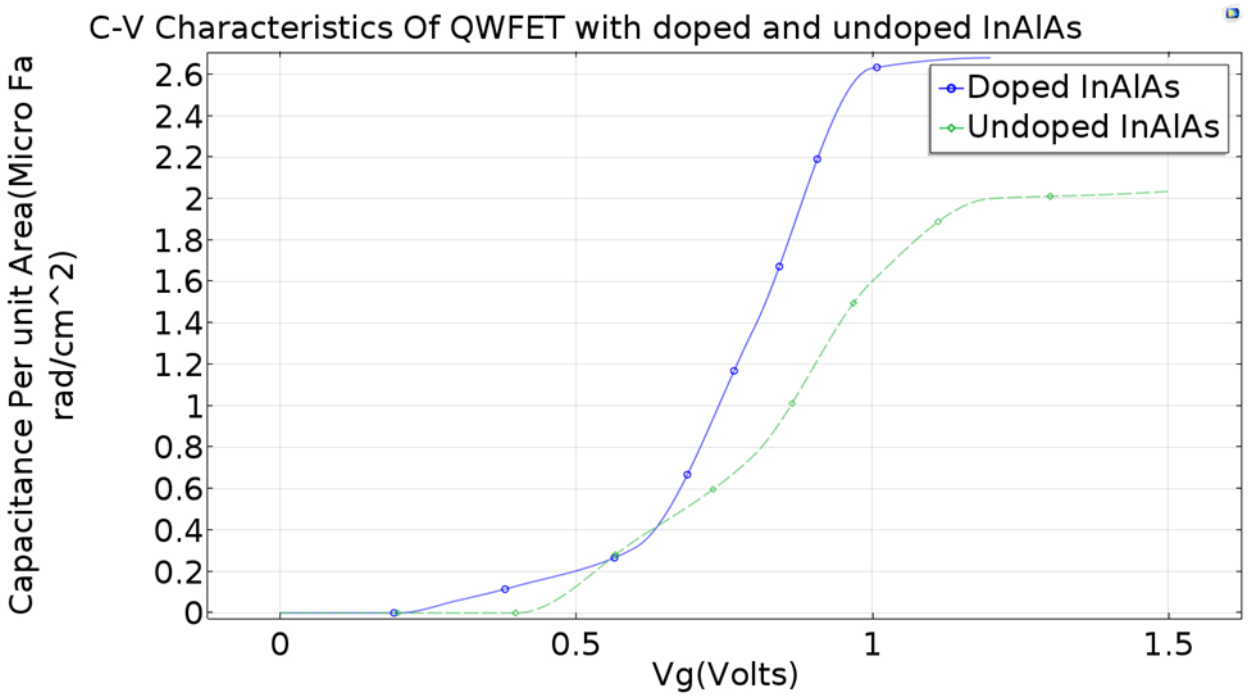

Fig 8.2.9: Comparison of C-V characteristics of QWFET with doped and undoped InAlAs

Finally, we compare the C-V characteristics of QWFETS with doped InP and InAlAs as upper barriers:

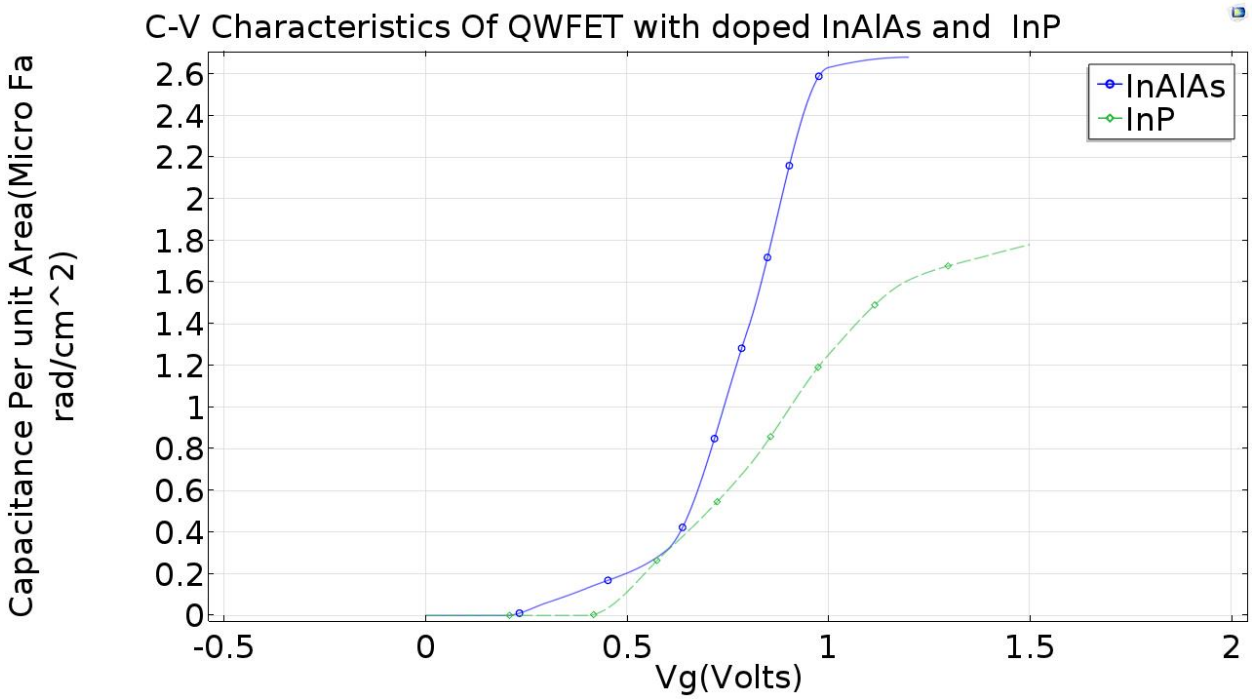

Fig 8.2.10: Comparison C-V characteristics of QWFET with doped InAlAs and doped InP

Finally, we can conclude that InAlAs is the more preferable material for use as the upper barrier than InP as it provides a much better yield for capacitance at the same voltage levels. So it is recommended to further research on QWFETs with InAlAs as the upper barrier to get even better yields from the devices.

9. FURTHER IMPROVEMENTS

In this paper, we have simulated the device by changing just two aspects of it, namely the material used in the upper barrier and the doping. Undoubtedly, if other factors were investigated as well, such as the oxide thickness, better results might have been achieved. Hence, we plan to carry on such research and employ more simulations in the near future.

REFERENCES

[1] C. H. Museum, "1960: Metal oxide semiconductor (MOS) transistor demonstrated,". [Online]. Available: http://www.computerhistory.org/siliconengine/metal-oxide-semiconductor-mos-transistor-demonstrated/. Accessed: Aug. 17, 2016.

[2] T. Mimura, "The early history of the high electron mobility transistor (HEMT)," IEEE Transactions on Microwave Theory and Techniques, vol. 50, no. 3, pp. 780–782, Mar. 2002.

[3] D. Kanter, "What's next for Moore's law? For Intel, III+V = 10nm QWFETs," 2015. [Online]. Available: http://www.realworldtech.com/intel-10nm-qwfet/. Accessed: Jun. 10, 2016.

[4] E. W. Weisstein, "Schrödinger equation -- from Eric Weisstein's world of physics," Wolfram Research, 1996.

[5] P. T. Center, "PTC Website," 2016. [Online]. Available: http://www.ece.ust.hk/~ptc/research.php?action=EDHEMT. Accessed: Aug. 7, 2016.

[6] L. Yang, C. Cheng, M. Bulsara and E. Fitzgerald, "High mobility In0.53Ga0.47As quantum-well metal oxide semiconductor field effect transistor structures," Journal of Applied Physics, pp. vol. 111, 104511, 2012.

[7] N. Chevillon, J.-M. Sallese, C. Lallement, F. Prégaldiny, M. Madec, J. Sedlmeir and J. Aghassi, "Generalization of the Concept of Equivalent Thickness and Capacitance to Multigate MOSFETs Modeling," IEEE Transactions on Electron Devices, vol. 59, no. 1, pp. 60 - 71, 2012.

[8] R. W. Pryor, Multiphysics modeling using COMSOL: A First principles approach. Sudbury, MA, United States: Jones and Bartlett Publishers, 2009.

[9] S. Jahangir and Q. D. M. Khosru, "A numerical model for solving two dimensional Poisson-Schrödinger equation in depletion all around operation of the SOI four gate transistor," 2009 IEEE International Conference of Electron Devices and Solid-State Circuits (EDSSC), Dec. 2009.

[10] Introduction to COMSOL Multiphysics Manual, COMSOL, 2015.

[11] Materials Library User's Guide, COMSOL, 2015.

[12] O. C. Zienkiewicz, 'The Finite Element Method', McGraw-Hill, London (1977)

[13] S. Datta, Quantum Transport: Atom to Transistor, Cambridge University Press, 2005.

[14] "NSM archive - physical properties of semiconductors,". [Online]. Available: http://www.ioffe.ru/SVA/NSM/Semicond/. Accessed: Aug. 16, 2016.

[15] M. Radosavljevic, G. Dewey, J. M. Fastenau, J. Kavalieros, R. Kotlyar, B. Chu-Kung, W. K. Liu, D. Lubyshev, M. Metz, K. Millard, N. Mukherjee, L. Pan, R. Pillarisetty, W. Rachmady, U. Shah, and R. Chau, "Non-planar, multi-gate InGaAs quantum well field effect transistors with high-K gate dielectric and ultra-scaled gate-to-drain/gate-to-source separation for low power logic applications," 2010 International Electron Devices Meeting, 2010.

[16] researchgate2016-, "Share and discover research," 2008. [Online]. Available: https://www.researchgate.net. Accessed: Aug. 16, 2016.

[17] D. A. Neamen, Semiconductor Physics and Devices, McGraw Hill, 2003.

[18] M. N. O. Sadiku, Elements of electromagnetics, 5th ed. New York: Oxford University Press, 2010.

[19] B. G. Streetman and S. K. Banerjee, Solid state electronic devices, 7th ed. United States: Prentice Hall, 2014.

[20] S. Datta, Lessons from Nanoelectronics: A new perspective on transport. Singapore, Singapore: World Scientific Publishing Co Pte, 2012.